# Accepted Manuscript


Development of novel amide–derivatized 2,4-bispyridyl thiophenes as highly potent and selective Dyrk1A inhibitors. Part II: Identification of the cyclopropylamide moiety as a key modification

Sarah S. Darwish, Mohammad Abdel-Halim, Ahmed K. ElHady, Mohamed Salah, Ashraf H. Abadi, Walter Becker, Matthias Engel

PII: S0223-5234(18)30769-4

DOI: 10.1016/j.ejmech.2018.08.097

Reference: EJMECH 10708

To appear in: *European Journal of Medicinal Chemistry*

Received Date: 14 June 2018

Revised Date: 29 August 2018

Accepted Date: 31 August 2018

Please cite this article as: S.S. Darwish, M. Abdel-Halim, A.K. ElHady, M. Salah, A.H. Abadi, W. Becker, M. Engel, Development of novel amide–derivatized 2,4-bispyridyl thiophenes as highly potent and selective Dyrk1A inhibitors. Part II: Identification of the cyclopropylamide moiety as a key modification, *European Journal of Medicinal Chemistry* (2018), doi: 10.1016/j.ejmech.2018.08.097.

**Graphical Abstract**

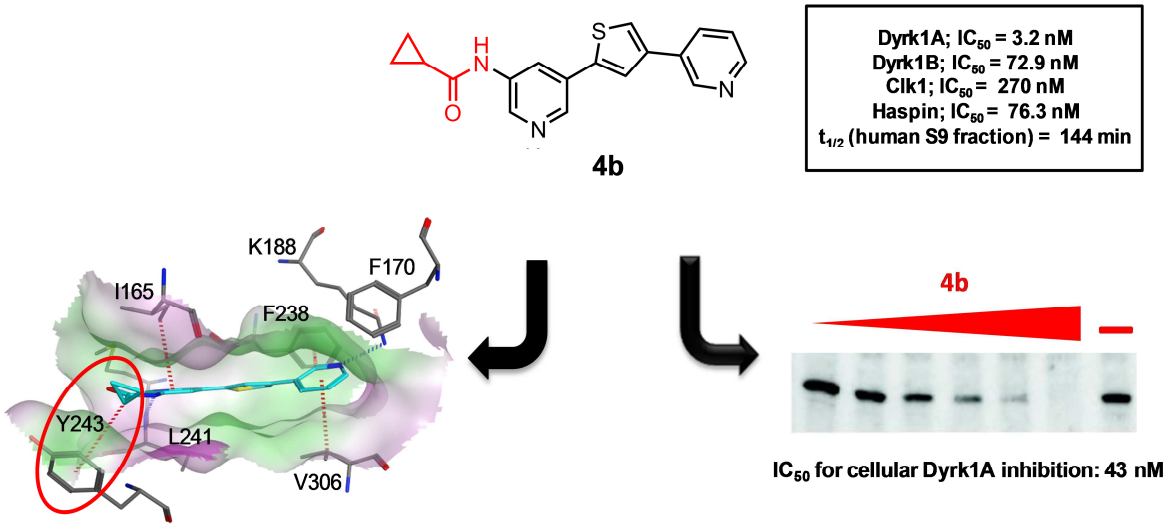

# Development of novel amide–derivatized 2,4-bispyridyl thiophenes as highly potent and selective Dyrk1A inhibitors. Part II: Identification of the cyclopropylamide moiety as a key modification

AUTHOR NAMES

*Sarah S. Darwish[1], Mohammad Abdel-Halim[1], Ahmed K. ElHady[1], Mohamed Salah[2], Ashraf H. Abadi[1], Walter Becker[3] and Matthias Engel[2]*

AUTHOR ADDRESS

[1]Department of Pharmaceutical Chemistry, Faculty of Pharmacy and Biotechnology, German University in Cairo, Cairo 11835, Egypt

[2]Pharmaceutical and Medicinal Chemistry, Saarland University, Campus C2.3, D-66123 Saarbrücken, Germany

[3]Institute of Pharmacology and Toxicology, Medical Faculty of the RWTH Aachen University, Wendlingweg 2, 52074 Aachen, Germany

**Abstract**

Dual-specificity tyrosine phosphorylation-regulated kinase 1A (Dyrk1A) is a potential target in Alzheimer's disease (AD) because of the established correlation between its over-expression and generation of neurofibrillary tangles (NFT) as well as the accumulation of amyloid plaques. However, the use of Dyrk1A inhibitors requires a high degree of selectivity over closely related kinases. In addition, the physicochemical properties of the Dyrk1A inhibitors need to be controlled to enable CNS permeability. In the present study, we optimized our previously published 2,4-bispyridyl thiophene class of Dyrk1A inhibitors by the synthesis of a small library of amide derivatives, carrying alkyl, cycloalkyl, as well as acidic and basic residues. Among this library, the cyclopropylamido modification (compound **4b**) was identified as being highly beneficial for several crucial properties. **4b** displayed high potency and selectivity against Dyrk1A over closely related kinases in cell-free assays ($IC_{50}$: Dyrk1A = 3.2 nM; Dyrk1B = 72.9 nM and Clk1 = 270 nM) and inhibited the Dyrk1A activity in HeLa cells with high efficacy ($IC_{50}$: 43 nM), while no significant cytotoxicity was observed. In addition, the cyclopropylamido group conferred high metabolic stability and maintained the calculated physicochemical properties in a range compatible with a potential CNS activity. Thus, based on its favourable properties, **4b** can be considered as a candidate for further *in vivo* testing in animal models of AD.

Keywords: Dyrk1A, neurodegenerative diseases, cyclopropyl amide, SF3b1 phosphorylation, CNS penetration

## 1 Introduction

Dual-specificity tyrosine-regulated kinases (Dyrks) belong to the larger human kinome family known as the CMGC group[1] which includes cyclin-dependent kinases (**C**DKs), mitogen-activated protein kinase (**M**APKs), glycogen synthase kinases (**G**SKs), and cdc-like kinases (**C**lks).[2] The Dyrk family comprises the mammalian subtypes 1A, 1B, 2, 3, and 4.[3] As their name implies, dual specificity kinases are capable of catalyzing their self-activation by autophosphorylation at a conserved tyrosine residue, whereas the resulting mature forms of the kinases can only phosphorylate exogenous protein substrates at serine or threonine residues.[1, 2] Due to its location in the Down Syndrome (DS) critical region on human chromosome 21, Dyrk1A is the most studied isoform in its family.[4-6] During embryonic development, Dyrk1A plays an important role in neurogenesis as well as neuronal differentiation,[7] hence its about 1.5 fold overexpression in DS-affected individuals (trisomy 21) is believed to contribute to the neurodevelopmental alterations associated with DS. Moreover, dysregulated Dyrk1A activity was shown to play a pathogenic role in the development of Alzheimer's disease (AD) in DS individuals.[1, 8] The main hallmarks of AD include neurofibrillary tangles (NFT) as well as the accumulation of amyloid plaques.[9] *In vitro* studies showed that Dyrk1A directly phosphorylates tau protein, leading to the loss of tau biological function as well as sequestration of normal tau and neurofibrillary degeneration.[10-12] Additionally, Dyrk1A was found associated with NFTs in individuals with DS in the age group of 38–51 years, suggesting that Dyrk1A contributes to the early onset of neurofibrillary degeneration.[13] Furthermore, over-expressed Dyrk1A hyperphosphorylates amyloid precursor protein (APP) which enhances the production of amyloid-β, the main component of amyloid plaques.[9, 13, 14]

More recently, evidence has accumulated that Dyrk1A can also contribute to α-synuclein aggregation and fibrillization in Lewy bodies in Parkinson's disease (PD) and Lewy body dementia. [15-19] Dyrk1A binds to and phosphorylates α-synuclein at Ser87.[15] In addition, Dyrk1A phosphorylates the neurodegeneration –related septin 4,[16] and complexes of these proteins may contribute to the cytoplasmic aggregation/fibrillization observed in PD, Lewy body dementia and multiple-system atrophy.[17, 18] Moreover, parkin was reported to co-localize and bind to Dyrk1A.[19] Dyrk1A directly phosphorylates parkin at Ser-131, causing the inhibition of its E3 ubiquitin ligase activity, which may also contribute to the pathogenesis of PD.

Furthermore, both AD and PD are also driven by aberrant splicing events which may be co-regulated by Dyrk1A, too.[20-23] Dyrk1A was reported to phosphorylate SR proteins which are considered among the main determinants of splice site recognition in pre-mRNA. [24] Dyrk1A is additionally known to catalyze the phosphorylation of the non-SR protein SF3b1 which is an important modulator of splicing reactions.[25] In AD, a misbalance of the two splicing–dependent 3R and 4R tau isoforms was shown to be caused by Dyrk1A in a mouse model.[26] This imbalance can be linked to the ability of Dyrk1A to phosphorylate relevant SR proteins such as SRp55, SC35 and ASF. [20-22] Besides the proven influence on the 3R/4R tau protein ratio, Dyrk1A over-dosage models also showed changes in the neuroligin mRNAs transcript composition as well as changes in the splicing pattern of acetylcholinesterase (AChE), leading to different AChE mRNA variants.[27]

Thus, pharmacological inhibition of Dyrk1A might not only suppress the pathogenic hyperphosphorylation of neuroproteins, it may also restore the normal pattern of splicing products of the respective proteins. In light of these pleiotropic functions of Dyrk1A,

potential pharmacological inhibitors of Dyrk1A should be highly selective to avoid the accumulation of adverse side effects due to additional off target inhibitions. Although many published Dyrk1A inhibitors, including harmine[28], INDY[29], leucettine L41[30], EHT 5372 [31], and 7-chloro-2-phenyl-1*H*-indole-3-carbonitrile[32] exhibited a good overall selectivity in a larger kinase screening panel, they still showed co-inhibition of at least one of the off-targets Dyrk1B, Clk1 and/or haspin, all of which show a high degree of similarity with Dyrk1A in their ATP binding site. The catalytic domain of Dyrk1A and Dyrk1B possess a sequence identity of 85%, and their ATP binding sites differ by only one amino acid residue: Met240 of Dyrk1A is replaced by Leu192 in Dyrk1B.[32] Dyrk1B was proposed as an anticancer target,[33-35] however, in the CNS, it was shown to be implicated in the regulation of astrocyte activation[36] which can have pro-inflammatory and neurotoxic but also neuroprotective roles.[37-39] In addition, prolonged inhibition of Dyrk1B may trigger or aggravate metabolic syndrome as a side effect, since the loss of Dyrk1B activity due to a point mutation that decreased the protein stability was shown to cause an autosomal-dominant form of metabolic syndrome.[40] Clk1 is involved in the regulation of alternative splicing,[41] too, hence co-inhibition of Dyrk1A and Clk1 might potentiate the effects on alternative splicing of numerous pre-mRNAs, which could be poorly tolerated during prolonged treatments. Finally, haspin is indispensable for cell division,[42] and its inhibition is expected to interfere with normal cell proliferation.

In a previous study, we introduced the 2,4-bispyridyl thiophene core as a favourable scaffold for Dyrk1A inhibition,[43] The selectivity of this scaffold over some of the common off target kinases was increased in a subsequent study using an amide–linked structural

extension.[44] In the current work, we present new derivatives of the 2,4-bispyridyl thiophene amides with further improved selectivity profiles and physicochemical properties.

## 2 Results and Discussion

### 2.1 Design strategy.

In our previous attempt to improve the selectivity towards Dyrk1A, we extended the bispyridyl thiophene scaffold by introducing an additional amino function on the pyridine at the thiophene-2 position, yielding compound **I** (compound **2** in ref.[44], Fig. 1). Its increased potency prompted us to attach a variety of side chains through amide linkage. In the library thus generated, we had identified Compound **II** (compound **31b** in ref.[44]) as the most potent inhibitor of that series. It also showed a great improvement in selectivity towards Dyrk1B and Clk1 ($IC_{50}$: Dyrk1B = 383 nM, Clk1 > 2µM, [ATP]=15 µM), however, we noticed that **II** still showed significant cross reactivity with haspin ($IC_{50}$ = 36 nM). In addition, the clogP value of the benzylamide derivative **II** (clogP = 4.11) was above the optimal average range reported for CNS active compounds, which is about 2.8.[45]

Therefore, it seemed straightforward to extend our diversification strategy by including mainly non aromatic and polar amide moieties, in order to enable alternative interactions with pocket side chains and decrease the lipophilicity. We selected different alkyl, cycloalkyl, as well as acidic and basic amide side chain extensions, which could potentially address pocket residues located at the hinge region of the ATP binding site (e.g., Tyr243 and Ile165) but also at the opposite side (e.g. Asp307, Phe170). We used the previously reported compound **I** as our extendable hit (Fig. 1).

## 2.2 Chemistry.

The main synthetic scheme for attaining the planned amide functionalized 2,4-bispyridyl thiophenes amide derivatives constitutes four steps (Scheme 1). Primarily, a Miyaura reaction was carried out on 3-amino-5-bromopyridine and bis(pinacolato)diboron in the presence of potassium acetate and Pd(dppf)$Cl_2$ as a catalyst to yield the corresponding boronic acid pinacol ester (Compound **A**). In the second step, Suzuki cross coupling reaction with 2,4-dibromothiophene in the presence of $Cs_2CO_3$ and palladium-tetrakis(triphenylphosphine) to give 4-bromothiophen-2-yl pyridine amines takes place to yield compound **B**. Afterwards, the amino group in compound **B** undergoes a coupling reaction with diverse carboxylic acids and methylsulfonyl chloride to yield a series of amides and sulfonamide, respectively. Finally, the free bromo in the previous amides/sulfonamides make the compounds accessible for a second Suzuki reaction with 3-pyridine boronic acid to synthesize the bispyridyl thiophene functionalized amides (**1b**-**8b**). Alkylation of the secondary amide of compound **4a** was done by deprotonation of the amide with KH followed by the reaction with the respective alkyl iodide then the product was coupled with 3-pyridine boronic acid to yield compounds **9**-**10** (Scheme 1). To have an amide with basic side chains, either an additional BOC deprotection was performed on compound **7b** using TFA to release compound **11** (Scheme 2) or the chloroacetamide derivative (compound **E**) was reacted with the appropriate alicyclic amines followed by subsequent Suzuki coupling to yield compounds **12**-**13** (Scheme 3). In order to omit the terminal pyridyl of compound **4b**, compound **B** was coupled with 2-bromothiophene, followed by amide coupling with cyclopropyl carboxylic acid to give compound **14** (Scheme 4). In addition to the compounds mentioned above, a second unique cluster of compounds was synthesized by linking the pyrazol-4-yl moiety to position 4 of the thiophene core of compound **4a.** In compounds**17**-**19**,

the 4-pyrazoleboronic acid pinacol ester was initially alkylated by its reaction with the corresponding alkyl iodides in the presence of $Cs_2CO_3$as a base (Scheme5).

### 2.3 Biological evaluation.

#### 2.3.1 Investigation of the amide linker.

Firstly, we investigated which type of amide was preferred as linking functionality with small alkyl groups. Comparing the methyl amide and the methyl sulfonamide derivatives (compounds **1b** and **2b**, respectively) of precursor compound **I** (Fig. 1), we found that the amide linkage was better tolerated (Table 1), although the activity of **1b** fell below that of **I**. However, an initial loss of potency was not unexpected for the simple amide derivative, because the mesomeric effect of the former amine was strongly diminished, thus lowering the electron density and H-bond acceptor strength at the pyridine nitrogen.

#### 2.3.2 The effect of alkylamido extensions.

Since the Dyrk1A inhibitory activity was totally abolished with the methyl sulfonamide (**2b**, Table 1), further alkyl extensions were subsequently introduced *via* the carboxamide linker, hoping to over-compensate the drop of potency brought about this functional group. While a simple homologation did not seem promising, as indicated by the lack of potency gain with the ethyl amide derivative **3b** (Table 1), the cyclopropyl substituent in compound **4b** caused a dramatic and unexpected increase in activity, lowering the $IC_{50}$ to 3.2 nM. Interestingly, a one-atom ring expansion through the use of cyclobutyl in compound **5b** reduced the inhibitory activity by more than 18-fold (Table 1). This trend was confirmed with larger cycloalkyl ring expansions, e. g., with the cyclohexyl derivative **6b** (40.3% inhibition at 250 nM), indicating that the cyclopropyl amide moiety in **4b** had the optimal size. It is likely that larger cycloalkyl rings

caused steric clashes with the predicted binding site at the ATP binding pocket (cf. below and Fig. 2).

### 2.3.3 The effect of polar and ionizable amide extensions.

Despite the large boost of potency observed with the cyclopropyl moiety, our further attempts focused on establishing polar interactions with the hydrophilic amino acid residues at the pocket border. Especially the introduction of basic moieties seemed worthwhile with respect to a potential enhancement of the CNS availability of our inhibitors – besides a general improvement of drug-like characteristics. The pyrrolidine-3-carboxamide derivative **11**, in which a secondary amine was integrated in the cycloalkylamide moiety, indicated some degree of tolerance toward basic functions, but did not reach by far the potency of the best compound, **4b** (Table 1). Shifting the position of the protonable nitrogen and introducing a methylene spacer, as in the piperidinylacetamide **12**, decreased the biological activity against Dyrk1A to the level of the cyclohexane carboxamide **6b**. The morpholino analogue **13** exhibited a further drop of activity, indicating that multiple polar atoms are not tolerated. A tetrazolyl acetamide derivative with reversed, partially anionic charge was also synthesized and tested (**8b**); its low inhibitory activity (24% at 250 nM) suggested that an anionic charge cannot compensate for the unfavourable influence of increased polarity (Table 1). Compound **7b**, the protected synthetic precursor of **11**, was also tested to probe whether a further structural extension by bulky side chains could be promising; however, this was not the case, as indicated by the total loss of activity with **7b**.

### 2.3.4 The effect of N-alkylation of the cyclopropylamide moiety.

Two more derivatives were synthesized by the N-alkylation of our most potent compound **4b** to afford the N-methyl and N-ethyl derivatives (compounds **9** and **10,** respectively). Both tertiary amide derivatives almost lost the Dyrk1A inhibitory activity (Table 1). N-alkylation of an amide

function not only removes the H-bond acceptor hydrogen, but also has a considerable impact on the preferred conformation, hydrophobicity and rotational flexibility of the respective molecule part. Most likely, the N-alkyl caused the carboxamide function to rotate out of the pyridine ring plane, due to steric hindrance between the alkyl and the *ortho* H atoms, thus stabilizing a biologically less active conformation. In our binding model, compound **4b** bound with a coplanar carboxamide–pyridine conformation (cf. Fig. 2). On the other hand, the loss of the HBD function did not play a role, at least according to our predicted binding model. Nevertheless, to exclude experimentally that an alternative binding mode could be formed, involving tandem H-bonding of the pyridine N and the amide carbonyl or NH to the hinge region, we synthesized the truncated derivative **14**, which should adopt this hypothetical binding mode more easily than the full length parent compound **4b**. As indicated by the complete loss of activity of **14**, the compounds did not switch to a new binding mode driven by tandem H-bonding to the hinge region, rather the 4-pyridyl ring was still essential, probably interacting with Lys188 as illustrated in Fig. 2.

### 2.3.5 Replacement of the 4-pyridyl in 4b by pyrazole.

With the last set of compounds, we investigated whether the nitrogen in a heteroaromatic five-membered ring could further increase the potency. In our previously reported series, the methyl pyrazole moiety proved to be a good surrogate of ring B as shown in compound **C30** in Fig. 1 (compound **30** in Ref.[43]), since it mediated a higher potency towards Dyrk1A than the 4-pyridyl in **C4** (compound 4 in Ref. [43], Fig. 1) ($IC_{50}$´s: 130 nM *vs.* 300 nM). Hence, it was straightforward to combine the favourable cyclopropylamide feature (this work) with the methyl pyrazolyl ring (previous work). The resulting compound **16** was also potent against Dyrk1A ($IC_{50}$=42.6 nM, Table 2), still exhibiting a 3-fold increase in potency compared to compound

**C30** due to the cyclopropyl amide extension. However, when compared to **4b**, compound **16** was almost 13-fold less potent, indicating that in the presence of the cyclopropylamide extension, pyridine was preferred as ring B (cf. Fig. 1) over N-methyl pyrazole. This was partially attributable to a steric hindrance of the N-methyl group in **16**, because the demethylated 1*H*-pyrazolyl derivative **15** was clearly more potent ($IC_{50}$ = 18 nM, Table 2).

Nevertheless, we aimed at exploring the possibility of utilizing the pyrazole nitrogen as a convenient attachment point for further molecule extensions. Therefore, we probed the effect of installing ethyl, propyl and isopropyl groups at the pyrazole N1 (compounds **17**, **18** and **19**, respectively). Interestingly, placing an ethyl group instead of the methyl in compound **16** slightly improved the inhibitory potency (compound **17,** $IC_{50}$ = 29.7 nM), suggesting that an enhancement of the hydrophobic effect partially compensated for the steric hindrance. However, further elongation of the alkyl chain to n-propyl (**18**) reduced the inhibitory activity again ($IC_{50}$=76 nM). Moreover, the branched isopropyl derivative (**19**) was almost inactive against Dyrk1A. These data suggested that pyrazole N1 in **15** was not suitable for molecule extensions because of the unfavourable vector, probably causing steric clashes of the substituents inside the binding pocket. In addition, a further disadvantage of the pyrazole containing scaffold was noted with respect to the selectivity. In general, the scaffold was better tolerated by Dyrk1B, thus lowering the selectivity factor for Dyrk1A over Dyrk1B to 8 for **15** (compared with 24 for **4b**), while the selectivity was even lost with the N-alkylated derivatives **16**–**18**. Fig. 3 summarizes the structure activity relationships of the current series toward Dyrk1A.

### 2.3.6 Predicted binding mode of 4b to Dyrk1A.

**4b** showed a remarkable boost of potency, which was attributable to the rather small cyclopropylamide moiety. To identify the binding mode of **4b** and the particular interactions of

the cyclopropylamide extension, we performed docking simulations to the ATP binding pocket using the coordinates from PDB entry 3ANR (human Dyrk1A/harmine complex). While in theory, binding in two different orientations was conceivable, each with the pyridine nitrogens forming H-bonds with Lys188 and the Leu241 NH, only one of the binding orientations placed the key cyclopropylamide group close to a pocket side chain with which it could interact (Fig. 2A). In this binding model, a CH-π interaction between the hinge region residueTyr243 and the cyclopropyl carbon in **4b** was observed. Furthermore, the cyclopropyl moiety showed packing against the Ile165 side chain, leading to additional hydrophobic interactions (Fig. 2B). Thus, the notable impact of the cyclopropyl may arise from a combination of CH–π and hydrophobic interactions with different side chains, leading to a synergistic enhancement of binding affinity. Such a cooperativity between different simultaneous interactions, also including hydrophobic interactions, is common in protein–ligand binding and has been experimentally confirmed.[46] Hence, if one of the specific interactions is weakened, the total binding affinity is over-proportionally affected. This might explain the low activity of **1b**; according to our docking model, the methyl at the amide function could also engage in CH–π interaction with Tyr243 but cannot reach Ile165 (see Fig. S1, Supplementary Information).

### 2.3.7 Selectivity against Dyrk1B and other selected kinases.

The selectivity of all new compounds was initially evaluated against Dyrk1B, the isoform most closely related to Dyrk1A, by screening at 250 nM, as shown in Tables 1 and 2. All of the new potent compounds were clearly more active against Dyrk1A, similar to what we observed with the benzamide and benzylamide derivatives.[44] The most potent cycloalkylamide derivatives of bispyridyl thiophene, **4b** and **5b**, showed selectivity factors (Dyrk1A over -1B) of approximately 24- and 4-fold, respectively. While the pyrazole analogue **15** also exhibited a significant 8-fold

selectivity toward Dyrk1A, this was lost with the N1-alkylated congeners (see above). Altogether, **4b** possessed the greatest selectivity for Dyrk1A in the present series, nearly approximating the 27 fold selectivity observed with the previous 4-fluorobenzyl amide derivative **II** (depicted in Fig. 1). To further examine the selectivity of **4b**, it was additionally tested against a panel of kinases (Table 3) which are supposed to have structurally similar ATP binding pockets and were frequently reported to show cross reactivity with diverse Dyrk1A inhibitors. As can be seen in Table 3, **4b** displayed a remarkable selectivity in this crucial selection of kinases, ranking **4b** among the most selective Dyrk1A inhibitors published so far. Even haspin, a kinase which was still slightly co-inhibited by the previous compound **II**, was 24 times less strongly inhibited by **4b** than the target Dyrk1A.

**How was the selectivity over the most closely related isoform Dyrk1B achieved?**

Despite the high sequence similarity between Dyrk1A and Dyrk1B, our most potent compound **4b** showed a remarkable 24 fold selectivity towards Dyrk1A. Indeed, the ATP binding sites of two closely related homologues differ only by a single amino acid (Met240 in Dyrk1A corresponds to Leu192 in Dyrk1B). Our docking model gave a hint on how this difference might translate into reduced affinity to Dyrk1B. Although the Met240 side chain in Dyrk1A is not directly facing the ATP binding pocket, it could be attracted by a hydrophobic patch created or enhanced upon binding of the inhibitor, thereby engaging in van der Waals and hydrophobic interactions with the pyridine ring in **4b** which is H-bonded to Leu241. The latter interactions could possibly contribute to anchoring the pyridine ring at this position in Dyrk1A, and might explain, at least partially, the lower potency of **4b** against Dyrk1B, where the van der Waals interaction surface to the corresponding Leu192 is considerably smaller (see Fig. 2B). Concomitantly, the essential H-bond of the pyridine N to the hinge region NH might be less

effectively shielded from water molecules in Dyrk1B. Furthermore, attractive interactions between aliphatic sulfur and pyridine nitrogen are well documented[47] and might play a role with Dyrk1A, but would be absent with Dyrk1B.

### 2.3.8 Inhibition of Dyrk1A in HeLa cells.

To evaluate the potency of **4b** against Dyrk1A in intact cells, we analyzed the effects on the intracellular phosphorylation of the splicing factor 3b1 (SF3b1) using western blot analysis (Fig. 4). The phosphorylation of Thr434 on SF3b1 was previously shown to be solely dependent on Dyrk1A activity in HeLa cells.[25] The inactive analogue **9** served as a negative control. In this assay, treatment of HeLa cells with **4b** reduced the pT343-signal in a concentration–dependent manner with an $IC_{50}$ value of 43 nM (Fig. 4). These results were in good agreement with the strong Dyrk1A inhibition observed in the cell free assay.

In parallel, we assessed the potential cytotoxicity of our most potent compound **4b** with the same cell line. As can be seen in Table 4, our test compounds showed minimal cytotoxicity on HeLa cells up to a concentration of 3 µM, which ensures the safety of our inhibitor in concentrations that fully inhibit Dyrk1A in cells.

## 2.4 Evaluation of CNS drug like properties.

Since the major indication for Dyrk1A inhibitors is the treatment of neurodegenerative diseases, it was straightforward to assess the ability of our novel analogues to cross the BBB. A set of physicochemical properties has been previously reported in literature to be associated with high probability of CNS penetration. [45] CNS–active drug candidates are assumed to have definite attributes exemplified in molecular weight: 181-427, logP: 0.4-5.1 (median: 2.8) ,[45] HBA: 2-3, HBD: 0-1, and TPSA (topological polar surface area) < 76 Å.[48] Accordingly, we calculated

different physicochemical parameters using ACD/Labs software for our most potent inhibitors (**4b** and **15b**) to estimate the CNS drug-likeness of the current series (Table 5). Most of the calculated parameters for both inhibitors were in good agreement with the ideal ranges for brain penetration as reported in literature. In comparison to the analogue from the previous series, **II**, Compounds **4b** and **15** showed more favourable characteristics, such as reduced logP and molecular weight, thus increasing the likeliness to penetrate the BBB. With respect to the TPSA values which exceeded the limit of 76 $Å^2$, it should be mentioned that this depends on whether the thiophene sulphur is included in the calculation or not. Sulphur actually shows little polarity in the aromatic ring system, and thiophene is therefore often employed as bioisosteric replacement for benzene. Without counting the thiophene sulphur, the TPSA values for **4b** and **15** are 54.9 and 70.7 $Å^2$, respectively.

Interestingly, searching the literature for structurally similar compounds that had shown high brain penetration *in vivo*, we found a series of pyridine–containing glutamate receptor antagonists, e. g., 2-{2-[3-(pyridin-3-yloxy)phenyl]-2H-tetrazol-5-yl}pyridine,[49] that even showed a larger polar surface due to the central tetrazole core. Altogether, our assessment suggested a high probability of CNS penetration for our most potent compounds **4b** and **15**.

### 2.5 Evaluation of metabolic stability.

To further assess whether **4b** and **15** are suitable for *in vivo* studies, the phase I and phase II metabolic stability were measured using human hepatic liver S9 fractions. A definite set of samples were taken at defined time points, and the remaining percentage of parent compound was determined by LC-MS/MS. The calculated half-life times almost reached 2.5 h for **4b** and **15** (Table 6), indicating a high metabolic stability, which exceeded that of the previous

benzylamide–extended compound **II** (half-life against human S9 fraction: 118 min,[44] tested in parallel).

## 3 Conclusions

We developed a novel Dyrk1A inhibitor series of amide–functionalized bispyridyl thiophenes carrying different alkyl, cycloalkyl and polar side chains. In this series, the cyclopropyl amide in compound **4b** was identified as a key modification, which led to an enhancement of several essential properties. Firstly, **4b** exhibited the most potent Dyrk1A inhibition with an $IC_{50}$ of 3.2 nM. In addition, the cyclopropyl amide modification effected a significant increase in selectivity over closely related kinases including haspin (selectivity factor: 24), which was often found to be co-inhibited even by some of the most selective Dyrk1A inhibitors, such as TG003 and harmine.[50, 51] Of note, the benzylamide–modified previous inhibitor **II** had only achieved a moderate 2.5 fold selectivity over haspin.[44] The cyclopropylamide modification did not only increase potency and selectivity, but moreover, it also enhanced the metabolic stability against human liver S9 fractions, leading to a half-life of almost 2.5 h.

As anticipated by the high cell free potency, **4b** inhibited Dyrk1A in HeLa cells with an $IC_{50}$ of only 43 nM. This cellular potency, in combination with the high selectivity, low cytotoxicity and high metabolic stability render **4b** a promising candidate for *in vivo* studies using models of neurodegenerative diseases.

## 4 Experimental Section

### 4.1 Chemistry.

Solvents and reagents were obtained from commercial suppliers and used as received. Melting points were determined on a Stuart SMP3 melting point apparatus. All final compounds had a percentage purity of at least 95%, and this could be verified by means of HPLC coupled with mass spectrometry. Mass spectra (HPLC−ESIMS) were obtained using a TSQ quantum (Thermo Electron Corp.) instrument prepared with a triple quadrupole mass detector (Thermo Finnigan) and an ESI source. All samples were injected using an autosampler (Surveyor, Thermo Finnigan) by an injection volume of 10 μL. The MS detection was determined using a source CID of 10 V and carried out at a spray voltage of 4.2 kV, a nitrogen sheath gas pressure of $4.0 \times 10^5$ Pa, a capillary temperature of 400 °C, a capillary voltage of 35 V, and an auxiliary gas pressure of $1.0 \times 10^5$ Pa. The stationary phase used was an RP C18 NUCLEODUR 100-3 (125 mm × 3 mm) column (Macherey & Nagel). The solvent system consisted of water containing 0.1% TFA (A) and 0.1% TFA in acetonitrile (B). The HPLC method used a flow rate of 400 μL/min. The percentage of B started at 5%, was increased up to 100% during 7 min, was kept at 100% for 2 min, and was flushed back to 5% in 2 min and was kept at 5% for 2 min. A Bruker DRX 500 spectrometer was used to obtain the $^1$H NMR and $^{13}$C NMR spectra. The chemical shifts are referenced to the residual protonated solvent signals.

#### 4.1.1 General synthetic procedures and experimental details.

##### 4.1.1.1 Procedure A, Procedure for synthesis of Compounds A-B, H.

A mixture of 5 mmol of the 3-amino-5-bromo pyridine and 1.96 gm (20 mmol) of potassium acetate and 0.18 gm (0.25 mmol) of $Pd(dppf)Cl_2$ and 5.08 gm (20 mmol) of bis(pinacolato)diboron in dioxane was heated to reflux under argon for 2 hours to yield

compounds **A**. The mixture was left to attain room temperature and then filtered under vacuum. Without further purification, a reaction flask containing the filterate was charged with 6.5 gm (20 mmol) of $Cs_2CO_3$, 0.29 gm (0.25 mmol) of palladium-tetrakis(triphenylphosphine) and 6 mmol of the appropriate bromothiophene together with 30% water in a Suzuki coupling reaction. The reaction was left to reflux under argon for 3.5 hours. The mixture was concentrated *in vacuo.* The residue was partitioned between 150 mls ethyl acetate and 50 mls brine solution and then the aqueous layer was re-extracted using 3 portions of 100 mls ethyl acetate. The organic layers were collected and the volume was reduced under reduced pressure. Afterwards the product was purified by CC to yield compounds **B, H**.

#### 4.1.1.2 Procedure B, General procedure for the amide synthesis of compounds 1a, 3a - 8a, E, 14.

0.18 gm **(**0.7 mmole) of compound **D** was added to a mixture of 0.4 gm (1.05 mmol) of HBTU (in compounds **1a**, **3a-7a, E, 14**) or 0.4 gm (1.05 mmol) HATU (in compounds **8a**) and 0.36 gm (1.05 mmol) of DIPEA together with 2.1 mmol of the appropriate acid in DCM. The mixture was left to stir at room temperature overnight, and afterwards, the solvent was evaporated *in vacuo* and the product was purified by CC.

#### 4.1.1.3 Procedure C, General procedure for amide alkylation (C– D)

0.14 gm (3.5 mmol) KH was added gradually to stirred solution of 0.23 gm (0.35 mmol) of compound **4a** in 2 mls DMF under ice cooling. The reaction mixture was left to stir for one hour and then 1 equiv of the appropriate alkyl iodide was added to the reaction vessel and the mixture was left to stir for 2 days at room temperature. The mixture was partitioned between aqueous brine solution and ethyl acetate layers and the aqueous layer was extracted by three 50-ml

portions of ethyl acetate. The organic layers were collected and the solvent was removed under vacuum, this was followed by purification of the desired products using CC.

#### 4.1.1.4 Procedure D, General procedure for synthesis of compounds F – G.

0.27 gm (0.7 mmol) of **compound E** was added to a solution of 7 mmol of the appropriate alicyclic amine dissolved in methanol. The reaction mixture was heated to refux for 1 hour. Afterwards, the solvent was removed *in vacuo* and the produced residue was purified using CC.

#### 4.1.1.5 Procedure E, General procedure for synthesis of compounds 1b–8b, 9-10, 12-13, 15-19.

The bromo derivative was added to a suspension of 4 equiv of $Na_2CO_3$ and 5 mmol% of $Pd(dppf)Cl_2$ in dioxane/water mixture. This was followed by the addition of the pyridine/pyrazole boronic acid derivative. The reaction was heated to reflux for 2 hours under argon atmosphere. The solvent was removed *in vacuo.* Small amount of brine solution was added and extraction was done using ethyl acetate (3 x 50 mls). The ethyl acetate portions were collected and the volume was reduced *in vacuo*. Afterwards the product was purified by CC

#### 4.1.1.6 Procedure F, General Procedure for pyrazole alkylation (compounds I, J, K)

To a solution of 4-pyrazoleboronic acid pinacol ester dissolved in acetone, 2 equiv of $Cs_2CO_3$ and 2 equiv of the appropriate alkyl iodide were added. The reaction mixture was left to reflux overnight. The solvent was evaporated *in vacuo* and the product entered the following reaction without further purification

**4.1.1.7 5-(4-Bromothiophen-2-yl)pyridin-3-amine (B).** The compound was synthesized according to Procedure **A**: yield 80%. The product was purified by CC (ethyl acetate); $^1$H NMR (500 MHz, DMSO) δ 8.08 (d, *J* = 2.0 Hz, 1H), 7.91 (d, *J* = 2.5 Hz, 1H), 7.70 (d, *J* = 1.4 Hz, 1H),

7.51 (d, *J* = 1.5 Hz, 1H), 7.16 – 7.05 (m, 1H), 5.50 (s, 2H); $^{13}$C NMR (126 MHz, DMSO) δ 144.98, 142.31, 136.28, 133.61, 128.34, 126.16, 123.47, 115.68, 109.89; MS (ESI) m/z = 254.82 $(M+H)^+$

**4.1.1.8 *N*-(5-(4-Bromothiophen-2-yl)pyridin-3-yl)-*N*-methylcyclopropanecarboxamide (C).** The compound was synthesized according to Procedure **C** using methyl iodide: yield 83%. The product was purified by CC (DCM/MeOH 100:1.5); $^1$H NMR (500 MHz, DMSO) δ 8.86 (s, 1H), 8.57 (d, *J* = 1.9 Hz, 1H), 8.19 (s, 1H), 7.83 (d, *J* = 1.4 Hz, 1H), 7.81 (d, *J* = 1.3 Hz, 1H), 3.34 (s, 3H), 1.54 – 1.37 (m, 1H), 0.86 – 0.82 (m, 2H), 0.69 (t, *J* = 4.3 Hz, 2H); $^{13}$C NMR (126 MHz, DMSO) δ 172.32, 147.61, 144.17, 140.69, 140.12, 130.89, 129.22, 127.99, 124.84, 110.20, 36.93, 12.39, 8.24; MS (ESI) m/z =336.91 $(M+H)^+$

**4.1.1.9 *N*-(5-(4-Bromothiophen-2-yl)pyridin-3-yl)-*N*-ethylcyclopropanecarboxamide (D).** The compound was synthesized according to Procedure **C** using ethyl iodide: yield 79%. The product was purified by CC (DCM/MeOH 100:1); $^1$H NMR (500 MHz, DMSO) δ 8.88 (s, 1H), 8.51 (s, 1H), 8.15 (s, 1H), 7.83 (t, *J* = 1.8 Hz, 2H), 3.75 (s, 2H), 1.25 – 1.13 (m, 1H), 1.04 (t, 3H), 0.88 – 0.77 (m, 2H), 0.66 (s, 2H); $^{13}$C NMR (126 MHz, DMSO) δ 171.69, 148.59, 144.64, 140.00, 139.00, 131.89, 129.40, 128.11, 124.86, 110.22, 43.53, 12.98, 12.62, 8.17; MS (ESI) m/z =350.89 $(M+H)^+$

**4.1.1.10 *N*-(5-(4-Bromothiophen-2-yl)pyridin-3-yl)acetamide (1a).** The compound was synthesized according to procedure **B** using acetic acid: yield 98%.The product was purified by CC (ethyl acetate); $^1$H NMR (500 MHz, DMSO) δ 10.30 (s, 1H), 8.64 (dd, *J* = 3.1, 2.4 Hz, 2H), 8.29 (t, *J* = 2.2 Hz, 1H), 7.79 (d, *J* = 1.4 Hz, 1H), 7.66 (d, *J* = 1.4 Hz, 1H), 2.10 (s, 3H); $^{13}$C

NMR (126 MHz, DMSO) δ 169.23, 141.17, 140.57, 140.02, 136.16, 128.35, 127.07, 124.41, 121.90, 110.23, 23.95; MS (ESI) m/z = 297.95 $(M+H)^+$

**4.1.1.11 *N*-(5-(4-Bromothiophen-2-yl)pyridin-3-yl)methanesulfonamide (2a).** The title compound was synthesized through adding 1.4 mmol of the methanesulfonyl chloride to a stirred solution of 0.18 gm (0.7 mmol) of compound **B** dissolved in pyridine. The reaction was heated to 60°C and left overnight. This was followed by the removal of solvent *in vacuo*: yield 69.1%. The product was purified by CC (ethyl acetate); $^1$H NMR (500 MHz, DMSO) δ 10.16 (s, 1H), 8.68 (d, J = 2.0 Hz, 1H), 8.39 (d, J = 2.4 Hz, 1H), 7.81 (d, J = 1.4 Hz, 1H), 7.77 (t, J = 2.2 Hz, 1H), 7.71 (d, J = 1.5 Hz, 1H), 3.13 (s, 3H); $^{13}$C NMR (126 MHz, DMSO) δ 141.43, 140.71, 135.35, 133.06, 128.82, 127.53, 124.65, 122.78, 110.19, 40.11; MS (ESI) m/z = 331.69 $(M)^+$

**4.1.1.12 *N*-(5-(4-Bromothiophen-2-yl)pyridin-3-yl)propionamide (3a).** The compound was synthesized according to procedure **B** using propionic acid: yield 64%. The product was purified by CC (ethyl acetate/petroleum ether 8:2);$^1$H NMR (500 MHz, DMSO) δ 10.36 (s, 1H), 8.69 (s, 1H), 8.63 (s, 1H), 8.34 (t, J = 2.2 Hz, 1H), 7.79 (d, J = 1.4 Hz, 1H), 7.66 (d, J = 1.4 Hz, 1H), 2.39 (q, J = 7.5 Hz, 2H), 1.10 (t, J = 7.5 Hz, 3H).MS (ESI) m/z = 310.99 $(M+H)^+$

**4.1.1.13 *N*-(5-(4-Bromothiophen-2-yl)pyridin-3-yl)cyclopropanecarboxamide (4a).** The compound was synthesized according to procedure **B** using cyclopropanecarboxylic acid: yield 94%. The product was purified by CC (ethyl acetate/petroleum ether 6:4); $^1$H NMR (500 MHz, DMSO) δ 10.57 (d, *J* = 1.2 Hz, 1H), 8.66 (d, *J* = 2.3 Hz, 1H), 8.63 (d, *J* = 2.1 Hz, 1H), 8.32 (t, *J* = 2.2 Hz, 1H), 7.79 (d, *J* = 1.4 Hz, 1H), 7.66 (d, *J* = 1.4 Hz, 1H), 1.80 (dd, *J* = 12.4, 6.3 Hz, 1H), 1.46 (m, *J* = 21.2, 15.9, 10.8, 6.4 Hz, 2H), 1.30 – 1.11 (m, 2H); $^{13}$C NMR (126 MHz, DMSO) δ

175.51, 141.14, 140.41, 139.93, 136.13, 128.31, 127.02, 124.33, 121.86, 110.16, 14.56, 7.65; MS (ESI) m/z = 322.93 $(M+H)^+$

**4.1.1.14 *N*-(5-(4-Bromothiophen-2-yl)pyridin-3-yl)cyclobutanecarboxamide (5a).** The compound was synthesized according to procedure **B** using cyclobutanecarboxylic acid: yield 94.6%. The product was purified by CC (ethyl acetate/petroleum ether 7:3); $^1$H NMR (400 MHz, DMSO) δ 10.15 (s, 1H), 8.69 (d, *J* = 1.9 Hz, 1H), 8.63 (d, *J* = 1.9 Hz, 1H), 8.35 (s, 1H), 7.79 (d, *J* = 1.1 Hz, 1H), 7.66 (d, *J* = 1.2 Hz, 1H), 3.09 – 2.99 (m, 1H), 1.10 – 1.00 (m, 2H), 0.97 (td, *J* = 7.0, 1.7 Hz, 2H), 0.82 (dd, *J* = 15.2, 7.5 Hz, 2H); $^{13}$C NMR (101 MHz, DMSO) δ 173.82, 141.21, 140.44, 140.13, 136.26, 128.30, 127.04, 121.99, 116.94, 110.22, 24.59, 17.73; MS (ESI) m/z = 337 $(M+H)^+$

**4.1.1.15 *N*-(5-(4-Bromothiophen-2-yl)pyridin-3-yl)cyclohexanecarboxamide (6a).** The compound was synthesized according to procedure **B** using cyclohexanecarboxylic acid: yield 51%. The product was purified by CC (ethyl acetate/petroleum ether 6:4); $^1$H NMR (500 MHz, DMSO) δ 10.17 (s, 1H), 8.67 (d, *J* = 2.3 Hz, 1H), 8.62 (d, *J* = 2.1 Hz, 1H), 8.35 (t, *J* = 2.2 Hz, 1H), 7.78 (d, *J* = 1.4 Hz, 1H), 7.65 (d, *J* = 1.5 Hz, 1H), 2.36 (ddd, *J* = 11.6, 8.1, 3.5 Hz, 1H), 1.83 (d, *J* = 11.8 Hz, 2H), 1.80 – 1.73 (m, 2H), 1.41 (m, *J* = 12.4, 2.9 Hz, 2H), 1.34 – 1.11 (m, 4H); $^{13}$C NMR (126 MHz, DMSO) δ 175.14, 141.21, 140.40, 140.07, 136.33, 128.28, 127.01, 124.34, 121.88, 110.19, 44.82, 29.01, 25.36, 25.16; MS (ESI) m/z = 364.97 $(M+H)^+$

**4.1.1.16 *tert*-Butyl 3-((5-(4-bromothiophen-2-yl)pyridin-3-yl)carbamoyl)pyrrolidine-1-carboxylate (7a).** The compound was synthesized according to procedure **B** using *N*-Boc-pyrrolidine-3-carboxylic acid: yield 88%. The product was purified by CC (DCM/MeOH 100:3); $^1$H NMR (500 MHz, DMSO) δ 10.40 (s, 1H), 8.66 (dd, *J* = 6.6, 2.2 Hz, 2H), 8.32 (t, *J* = 2.2 Hz,

1H), 7.79 (d, *J* = 1.4 Hz, 1H), 7.67 (d, *J* = 1.4 Hz, 1H), 3.03 (dd, *J* = 16.4, 8.6 Hz, 2H), 2.13 (d, *J* = 2.9 Hz, 1H), 2.03 (s, 2H), 2.00 – 1.90 (m, 2H), 1.41 (s, 9H); $^{13}$C NMR (126 MHz, DMSO) δ 153.35, 141.06, 140.77, 140.20, 135.94, 132.94, 128.34, 127.11, 124.41, 122.19, 110.21, 78.34, 54.89, 53.55, 41.81, 28.16, 28.14; MS (ESI) m/z =453.84 $(M+H)^+$

**4.1.1.17 *N*-(5-(4-Bromothiophen-2-yl)pyridin-3-yl)-2-(1*H*-tetrazol-5-yl)acetamide (8a).** The compound was synthesized according to procedure **B** using 1*H*-Tetrazole-5-acetic acid: yield 97%. The product was purified by extraction with 2 M NaOH and ethyl acetate (3 X 50 mls). The aqueous layer was normalized using 1 M HCl and dried *in vacuo*; $^1$H NMR (500 MHz, DMSO) δ 10.78 (s, 1H), 8.68 (d, *J* = 2.3 Hz, 1H), 8.61 (d, *J* = 2.1 Hz, 1H), 8.33 (t, *J* = 2.2 Hz, 1H), 7.77 (d, *J* = 1.4 Hz, 1H), 7.64 (d, *J* = 1.4 Hz, 1H), 3.77 (s, 2H), 3.42 (s, 1H); $^{13}$C NMR (126 MHz, DMSO) δ 169.31, 155.55, 141.19, 140.54, 140.13, 136.22, 128.34, 127.08, 124.39, 121.97, 110.19, 34.83; MS (ESI) m/z = 364.90 $(M+H)^+$

**4.1.1.18 2-(Piperidin-1-yl)-*N*-(5-(4-(pyridin-3-yl)thiophen-2-yl)pyridin-3-yl)acetamide (F).** The compound was synthesized according to procedure **D** using piperidine: yield 83.8%. The product was purified by CC (ethyl acetate/MeOH 100:1); $^1$H NMR (500 MHz, DMSO) δ 9.81 (s, 1H), 8.61 (d, *J* = 2.3 Hz, 1H), 8.46 (d, *J* = 2.1 Hz, 1H), 8.16 (t, *J* = 2.2 Hz, 1H), 7.61 (d, *J* = 1.4 Hz, 1H), 7.49 (d, *J* = 1.4 Hz, 1H), 2.94 (s, 2H), 2.35 – 2.30 (m, 4H), 1.39 (m, *J* = 11.1, 5.6 Hz, 4H), 1.22 (d, *J* = 4.2 Hz, 2H); $^{13}$C NMR (126 MHz, DMSO) δ 164.59, 141.07, 140.84, 140.67, 135.52, 128.31, 127.14, 124.40, 122.64, 110.17, 62.55, 54.11, 25.32, 23.51; MS (ESI) = 379.96 $(M+H)^+$

**4.1.1.19 *N*-(5-(4-Bromothiophen-2-yl)pyridin-3-yl)-2-morpholinoacetamide (G).** The compound was synthesized according to procedure **D** using morpholine: yield 83.3%. The

product was purified by CC (ethyl acetate /MeOH 100:3); $^{1}$H NMR (500 MHz, DMSO) δ 10.07 (s, 1H), 8.78 (d, *J* = 2.2 Hz, 1H), 8.66 (d, *J* = 2.1 Hz, 1H), 8.34 (t, *J* = 2.2 Hz, 1H), 7.79 (d, *J* = 1.4 Hz, 1H), 7.68 (d, *J* = 1.4 Hz, 1H), 3.69 – 3.62 (m, 4H), 3.20 (d, *J* = 15.9 Hz, 2H), 2.52 (m, 4H); $^{13}$C NMR (126 MHz, DMSO) δ 169.13, 164.60, 141.06, 140.91, 135.51, 128.31, 127.14, 124.42, 122.73, 110.19, 66.02, 61.95, 53.18; MS (ESI) m/z = 383.86 $(M+H)^{+}$

**4.1.1.20 5-(Thiophen-2-yl)pyridin-3-amine (H**). The compound was synthesized according to Procedure **A** using 2-bromothiophene: yield 89%.The product was purified by CC (ethyl acetate/petroleum ether 9:1); $^{1}$H NMR (500 MHz, DMSO) δ 8.07 (d, *J* = 1.7 Hz, 1H), 7.87 (d, *J* = 2.3 Hz, 1H), 7.57 (d, *J* = 5.0 Hz, 1H), 7.46 (d, *J* = 3.2 Hz, 1H), 7.20 – 7.09 (m, 2H), 5.47 (s, 2H); $^{13}$C NMR (126 MHz, DMSO) δ 144.95, 140.69, 135.61, 133.80, 129.50, 128.47, 126.03, 124.03, 115.94.

**4.1.1.21 *N*-(5-(4-(Pyridin-3-yl)thiophen-2-yl)pyridin-3-yl)acetamide (1b).** The compound was synthesized according to procedure **E** to give a brown solid: yield 13.8%. The product was purified by CC (DCM/MeOH/TEA 100:5:1); mp151.3-153.2 °C; $^{1}$H NMR (500 MHz, DMSO) δ 10.50 (s, 1H), 9.06 (d, *J* = 1.7 Hz, 1H), 8.74 (d, *J* = 1.8 Hz, 1H), 8.69 (d, *J* = 2.0 Hz, 1H), 8.53 (d, *J* = 3.6 Hz, 1H), 8.38 (s, 1H), 8.19 (dd, *J* = 8.3, 4.6 Hz, 2H), 8.15 (s, 1H), 7.47 (dd, *J* = 7.9, 4.8 Hz, 1H), 2.11 (s, 3H); $^{13}$C NMR (126 MHz, DMSO) δ 169.25, 148.41, 147.21, 140.87, 140.64, 139.70, 139.39, 136.23, 133.31, 130.43, 129.27, 123.94, 123.68, 122.93, 122.09, 23.93; MS (ESI) m/z = 296.02 $(M + H)^{+}$

**4.1.1.22 *N*-(5-(4-(Pyridin-3-yl)thiophen-2-yl)pyridin-3-yl)methanesulfonamide (2b).** The compound was synthesized according to procedure **E** to give a white solid: yield 45.4%. The product was purified by extraction with water and ethyl acetate (3X50 mls) the organic layers

were collected and the solvent was removed *in vacuo*; mp >280 °C; $^{1}$H NMR (500 MHz, DMSO) δ 10.37 (s, 1H), 9.06 (s, 1H), 8.76 (d, *J* = 1.9 Hz, 1H), 8.53 (d, *J* = 3.4 Hz, 1H), 8.43 (d, *J* = 2.1 Hz, 1H), 8.21 (s, 2H), 8.17 (s, 1H), 7.89 (s, 1H), 7.47 (dd, *J* = 7.9, 4.6 Hz, 1H), 3.11 (s, 3H);$^{13}$C NMR (126 MHz, DMSO) δ 148.40, 147.19, 141.33, 140.68, 140.40, 139.53, 139.36, 135.86, 133.30, 130.37, 129.70, 124.06, 123.90, 123.17; MS (ESI) m/z = 331.79 $(M + H)^{+}$

**4.1.1.23 *N*-(5-(4-(Pyridin-3-yl)thiophen-2-yl)pyridin-3-yl)propionamide (3b).** The compound was synthesized according to procedure **E** to give a beige solid: yield 9.1%. The product was purified by CC (DCM/MeOH 100:5); mp 211.6-212.4 °C; $^{1}$H NMR (500 MHz, DMSO) δ 10.21 (s, 1H), 9.06 (d, *J* = 1.7 Hz, 1H), 8.73 (d, *J* = 2.1 Hz, 1H), 8.67 (d, *J* = 2.2 Hz, 1H), 8.53 (dd, *J* = 4.7, 1.5 Hz, 1H), 8.39 (t, *J* = 2.2 Hz, 1H), 8.19 (ddd, *J* = 8.0, 2.3, 1.6 Hz, 1H), 8.17 (d, *J* = 1.5 Hz, 1H), 8.13 (d, *J* = 1.4 Hz, 1H), 7.47 (ddd, *J* = 7.9, 4.8, 0.8 Hz, 1H), 2.39 (q, *J* = 7.5 Hz, 2H), 1.12 (t, *J* = 7.5 Hz, 3H); $^{13}$C NMR (126 MHz, DMSO) δ 172.79, 148.34, 147.17, 140.85, 140.53, 139.68, 139.36, 136.16, 133.24, 130.39, 129.23, 123.85, 123.61, 122.82, 122.07, 29.39, 9.37; MS (ESI) m/z = 310.08 $(M + H)^{+}$

**4.1.1.24 *N*-(5-(4-(Pyridin-3-yl)thiophen-2-yl)pyridin-3-yl)cyclopropanecarboxamide (4b).** The compound was synthesized according to procedure **E** to give a brick red solid: yield 8.5%. The product was purified by CC (DCM/MeOH 100:5); mp 194-195.8 °C; $^{1}$H NMR (500 MHz, DMSO) δ 10.58 (s, 1H), 9.06 (d, *J* = 1.9 Hz, 1H), 8.69 (dd, *J* = 37.5, 2.1 Hz, 2H), 8.52 (dd, *J* = 4.7, 1.4 Hz, 1H), 8.39 (t, *J* = 2.2 Hz, 1H), 8.23 – 8.16 (m, 2H), 8.13 (d, *J* = 1.4 Hz, 1H), 7.47 (dd, *J* = 7.9, 4.8 Hz, 1H), 1.85 – 1.78 (m, 1H), 0.95 – 0.79 (m, 4H); $^{13}$C NMR (126 MHz, DMSO) δ 172.53, 148.35, 147.15, 140.82, 140.52, 139.57, 139.35, 136.13, 133.24, 130.38, 129.26, 123.87, 123.63, 122.85, 122.03, 14.56, 7.56; MS (ESI) m/z = 321.93 $(M + H)^{+}$

**4.1.1.25 *N*-(5-(4-(Pyridin-3-yl)thiophen-2-yl)pyridin-3-yl)cyclobutanecarboxamide (5b).** The compound was synthesized according to procedure **E** to give an off-white solid: yield 17%. The product was purified by CC (DCM/MeOH 100:4); mp 213-214.2 °C; $^{1}$H NMR (500 MHz, DMSO) δ 10.09 (s, 1H), 9.06 (s, 1H), 8.73 (s, 1H), 8.68 (s, 1H), 8.53 (d, *J* = 4.0 Hz, 1H), 8.41 (s, 1H), 8.20 (d, *J* = 8.7 Hz, 2H), 8.14 (s, 1H), 7.47 (dd, *J* = 7.7, 4.7 Hz, 1H), 3.31 – 3.22 (m, 1H), 2.32 – 2.19 (m, 2H), 2.14 (d, *J* = 8.6 Hz, 2H), 1.96 (dd, *J* = 19.0, 9.3 Hz, 1H), 1.83 (d, *J* = 9.8 Hz, 1H); $^{13}$C NMR (126 MHz, DMSO) δ173.76, 148.38, 147.20, 140.87, 140.57, 139.78, 139.38, 136.21, 133.27, 130.42, 129.24, 123.89, 123.65, 122.86, 122.16, 24.58, 17.71; MS (ESI) m/z =336.08 $(M + H)^+$

**4.1.1.26 *N*-(5-(4-(Pyridin-3-yl)thiophen-2-yl)pyridin-3-yl)cyclohexanecarboxamide (6b).** The compound was synthesized according to procedure **E** to give a beige solid: yield 14%. The product was purified by CC (DCM/MeOH 100:3); mp 182-184 °C; $^{1}$H NMR (500 MHz, DMSO) δ 10.17 (s, 1H), 9.06 (s, 1H), 8.72 (s, 1H), 8.67 (s, 1H), 8.53 (d, *J* = 3.7 Hz, 1H), 8.42 (s, 1H), 8.23 – 8.15 (m, 2H), 8.13 (s, 1H), 7.53 – 7.42 (m, 1H), 2.38 (t, *J* = 11.4 Hz, 1H), 1.85 (d, *J* = 12.2 Hz, 2H), 1.77 (d, *J* = 11.9 Hz, 2H), 1.66 (d, *J* = 12.0 Hz, 1H), 1.43 (d, *J* = 12.2 Hz, 2H), 1.26 (dd, *J* = 23.2, 10.8 Hz, 2H), 1.22 – 1.16 (m, 1H) $^{13}$C NMR (126 MHz, DMSO) δ 175.08, 148.33, 147.16, 140.87, 140.49, 139.70, 139.35, 136.30, 133.25, 130.40, 129.20, 123.86, 123.59, 122.82, 122.03, 44.79, 29.00, 25.35, 25.15; MS (ESI) m/z = 364.03 $(M + H)^+$

**4.1.1.27 *tert*-Butyl 3-((5-(4-(pyridin-3-yl)thiophen-2-yl)pyridin-3-yl)carbamoyl)pyrrolidine-1-carboxylate (7b).** The compound was synthesized according to procedure **E** to give a yellow semi-solid: yield 34%. The product was purified by CC (DCM/MeOH/ TEA 100:4:1); $^{1}$H NMR (500 MHz, DMSO) δ 10.49 (s, 1H), 9.08 (s, 1H), 8.73 (dd, *J* = 32.1, 1.9 Hz, 2H), 8.55 (d, *J* = 3.5 Hz, 1H), 8.41 (t, *J* = 2.1 Hz, 1H), 8.27 – 8.21 (m, 1H), 8.20 (d, *J* = 1.4 Hz, 1H), 8.16 (d, *J* = 1.4

Hz, 1H), 7.51 (dd, *J* = 7.9, 4.8 Hz, 1H), 3.54 (dd, *J* = 20.8, 11.7 Hz, 2H), 3.25 – 3.16 (m, 2H), 2.10 (dd, *J* = 29.5, 14.7 Hz, 2H), 1.41 (s, 9H), 1.23 (d, *J* = 1.2 Hz, 1H); $^{13}$C NMR (126 MHz, DMSO) δ 177.88, 153.34, 147.97, 146.77, 140.80, 139.80, 139.22, 133.72, 130.57, 129.47, 129.15, 128.07, 124.07, 123.74, 123.10, 122.35, 78.38, 61.17, 45.66, 45.59, 28.20, 28.17; MS (ESI) m/z = 451.35 $(M + H)^+$

**4.1.1.28 *N*-(5-(4-(Pyridin-3-yl)thiophen-2-yl)pyridin-3-yl)-2-(1*H*-tetrazol-5-yl)acetamide (8b).** The compound was synthesized according to procedure **E** to give an off-white solid: yield 55.4%. The product was purified by CC (DCM/MeOH/TEA 100:11:3); mp 119.2-122.7 °C; $^1$H NMR (500 MHz, DMSO) δ 10.80 (s, 1H), 9.14 – 8.99 (m, 1H), 8.73 (d, *J* = 2.1 Hz, 1H), 8.69 (d, *J* = 2.2 Hz, 1H), 8.52 (dd, *J* = 4.7, 1.6 Hz, 1H), 8.40 (t, *J* = 2.2 Hz, 1H), 8.22 – 8.16 (m, 2H), 8.14 (d, *J* = 1.4 Hz, 1H), 7.50 – 7.43 (m, 1H), 5.32 (s, 1H), 3.86 (s, 2H); $^{13}$C NMR (126 MHz, DMSO) δ 172.10, 168.73, 148.35, 147.19, 140.80, 140.73, 139.73, 139.37, 136.12, 133.28, 130.42, 129.27, 123.89, 123.71, 122.89, 122.10, 34.34; MS (ESI) m/z = 364.02 $(M + H)^+$

**4.1.1.29 *N*-Methyl-*N*-(5-(4-(pyridin-3-yl)thiophen-2-yl)pyridin-3-yl)cyclopropanecarboxamide (9).** The compound was synthesized according to procedure **E** to give brown oil: yield 15.6%. The product was purified by CC (DCM/MeOH 100:2); mp 142-142.7 °C; $^1$H NMR (500 MHz, DMSO) δ 9.07 (s, 1H), 8.93 (s, 1H), 8.57 (s, 1H), 8.53 (d, *J* = 3.7 Hz, 1H), 8.34 (s, 1H), 8.25 (s, 1H), 8.20 – 8.16 (m, 2H), 7.48 (dd, *J* = 7.9, 4.8 Hz, 1H), 3.31 (s, 3H), 1.22 (m, 1H), 0.89 – 0.84 (m, 2H), 0.70 (m, 2H); $^{13}$C NMR (126 MHz, DMSO) δ 172.30, 149.12, 148.40, 147.76, 147.14, 140.71, 139.67, 139.28, 134.40, 133.18, 130.32, 124.67, 123.96, 123.89, 123.31, 36.97, 12.35, 8.20; MS (ESI) m/z = 336.03 $(M + H)^+$

**4.1.1.30 *N*-Ethyl-*N*-(5-(4-(pyridin-3-yl)thiophen-2-yl)pyridin-3-yl)cyclopropanecarboxamide (10).** The compound was synthesized according to procedure **E** to give a beige solid: yield 21.2%. The product was purified by CC (DCM/MeOH 100:3); mp 140-142.2 °C; $^{1}$H NMR (500 MHz, DMSO) δ 9.07 (d, *J* = 1.9 Hz, 1H), 8.94 (s, 1H), 8.58 – 8.44 (m, 2H), 8.36 (s, 1H), 8.24 – 8.19 (m, 2H), 8.18 (d, *J* = 1.3 Hz, 1H), 7.48 (dd, *J* = 7.8, 4.8 Hz, 1H), 3.78 (q, *J* = 6.3 Hz, 2H), 1.30 (m, 1H), 1.07 (t, *J* = 6.6 Hz, 3H), 0.88 – 0.81 (m, 2H), 0.67 (m, 2H); $^{13}$C NMR (126 MHz, DMSO) δ 171.81, 148.40, 148.17, 147.16, 144.66, 144.45, 139.55, 139.29, 139.02, 133.18, 131.82, 130.30, 124.79, 123.87, 123.32, 43.57, 12.99, 12.63, 8.15; MS (ESI) m/z =350.05 $(M + H)^{+}$

**4.1.1.31 *N*-(5-(4-(Pyridin-3-yl)thiophen-2-yl)pyridin-3-yl)pyrrolidine-3-carboxamide (11).** The title compound was prepared by adding **compound 7b** to a mixture of TFA and DCM. The reaction mixture was stirred overnight at room temperature and then the solvent was removed *in vacuo* and purified by crystallization from ethanol to give yellow oil: yield 23.6%. $^{1}$H NMR (500 MHz, MeOD)δ 8.97 (s, 1H), 8.66 (dd, *J* = 7.3, 1.8 Hz, 2H), 8.52 (d, *J* = 4.4 Hz, 1H), 8.47 (t, *J* = 2.2 Hz, 1H), 8.36 – 8.26 (m, 1H), 8.05 (s, 1H), 7.97 (dd, *J* = 3.7, 1.5 Hz, 2H), 7.61 (dd, *J* = 7.9, 5.1 Hz, 1H), 3.66 (dd, *J* = 11.7, 5.0 Hz, 1H), 3.49 (dd, *J* = 11.7, 7.7 Hz, 1H), 3.45 – 3.35 (m, 3H), 2.50 – 2.35 (m, 1H), 2.29 (m, *J* = 13.2, 5.9 Hz, 1H), 1.27 (dd, *J* = 14.8, 7.8 Hz, 1H); $^{13}$C NMR (126 MHz, MeOD) δ 173.24, 147.11, 146.14, 142.42, 142.07, 140.58, 140.04, 137.55, 137.47, 133.83, 132.00, 126.28, 125.31, 124.99, 124.79, 48.76, 46.56, 44.80, 30.38.; MS (ESI) m/z = 350.93 $(M + H)^{+}$

**4.1.1.32 2-(Piperidin-1-yl)-*N*-(5-(4-(pyridin-3-yl)thiophen-2-yl)pyridin-3-yl)acetamide (12).** The compound was synthesized according to procedure **E** to give brick red oil: yield 17.5%. The product was purified by CC (DCM/MeOH 100:3); $^{1}$H NMR (500 MHz, DMSO) δ 11.10 (s, 1H),

9.18 (s, 1H), 8.87 (s, 1H), 8.72 (s, 1H), 8.44 (d, *J* = 7.8 Hz, 1H), 8.37 (s, 1H), 8.27 (d, *J* = 8.0 Hz, 2H), 7.70 (s, 1H), 7.54 (d, *J* = 8.1 Hz, 1H), 4.20 (s, 2H), 3.51 (s, 2H), 3.09 (s, 2H), 1.80 (s, 4H), 1.70 (s, 1H), 1.40 (s, 1H); $^{13}$C NMR (126 MHz, DMSO) δ 163.87, 145.98, 144.77, 141.54, 140.51, 139.80, 138.44, 135.76, 130.95, 130.87, 128.49, 124.99, 124.05, 123.93, 122.75, 56.86, 53.09, 22.13, 20.97; MS (ESI) m/z = 379.09 $(M + H)^+$

**4.1.1.33 2-morpholino-*N*-(5-(4-(pyridin-3-yl)thiophen-2-yl)pyridin-3-yl)acetamide (13).** The compound was synthesized according to procedure **E** to give a buff yellow solid: yield 7.7%. The product was purified by CC (DCM/ MeOH 100:5); mp 174.3-175.8 °C; $^1$H NMR (500 MHz, DMSO) δ 11.47 (s, 1H), 9.09 (d, *J* = 1.8 Hz, 1H), 8.81 (dd, *J* = 29.4, 2.0 Hz, 2H), 8.56 (dd, *J* = 4.8, 1.3 Hz, 1H), 8.42 (t, *J* = 2.0 Hz, 1H), 8.28 (d, *J* = 8.2 Hz, 1H), 8.22 (dd, *J* = 17.6, 1.3 Hz, 2H), 7.54 (dd, *J* = 7.9, 4.8 Hz, 1H), 4.21 (s, 2H), 3.89 (s, 4H), 3.33 (s, 4H); $^{13}$C NMR (126 MHz, DMSO) δ 174.82, 146.42, 141.55, 140.47, 139.97, 139.13, 135.13, 134.09, 130.65, 129.39, 124.22, 123.91, 123.41, 122.76, 122.71, 51.99, 45.30, 8.39; MS (ESI) m/z = 381.07 $(M + H)^+$

**4.1.1.34 *N*-(5-(Thiophen-2-yl)pyridin-3-yl)cyclopropanecarboxamide (14).** The compound was synthesized according to procedure **B** using cyclopropanecarboxylic acid to give a brown solid: yield 45.4%. The product was purified by CC (DCM/MeOH 100:4); mp 149.8-151.1 °C; $^1$H NMR (500 MHz, DMSO) δ 10.50 (s, 1H), 8.64 (d, *J* = 2.3 Hz, 1H), 8.60 (d, *J* = 2.1 Hz, 1H), 8.32 (t, *J* = 2.2 Hz, 1H), 7.65 (dd, *J* = 5.1, 1.1 Hz, 1H), 7.58 (dd, *J* = 3.6, 1.2 Hz, 1H), 7.19 (dd, *J* = 5.1, 3.6 Hz, 1H), 1.88 – 1.76 (m, 1H), 0.90 – 0.78 (m, 4H); $^{13}$C NMR (126 MHz, DMSO) δ 172.46, 140.42, 139.55, 139.26, 136.12, 129.50, 128.70, 126.91, 124.88, 121.99, 14.55, 7.51; MS (ESI) m/z = 244.99 $(M + H)^+$

**4.1.1.35 *N*-(5-(4-(1H-pyrazol-4-yl)thiophen-2-yl)pyridin-3-yl)cyclopropanecarboxamide (15).** The compound was synthesized according to procedure **E** using 4-Pyrazoleboronic acid pinacol ester to give a white solid: yield 18.1%. The product was purified by CC (DCM/MeOH 100:4); mp 250-253.2; $^{1}$H NMR (500 MHz, DMSO) δ 12.91 (s, 1H), 10.55 (s, 1H), 8.64 (t, *J* = 2.2 Hz, 2H), 8.36 (t, *J* = 2.0 Hz, 1H), 8.16 (s, 1H), 7.89 (d, *J* = 1.0 Hz, 2H), 7.64 (d, *J* = 0.9 Hz, 1H), 1.82 (dd, *J* = 6.8, 3.9 Hz, 1H), 0.95 – 0.79 (m, 4H); $^{13}$C NMR (126 MHz, DMSO) δ 172.50, 140.33, 139.68, 139.33, 136.58, 136.14, 135.16, 129.53, 125.61, 124.01, 121.84, 118.48, 116.62, 14.56, 7.54; MS (ESI) m/z = 311.02 $(M + H)^+$

**4.1.1.36 *N*-(5-(4-(1-Methyl-1*H*-pyrazol-4-yl)thiophen-2-yl)pyridin-3-yl)cyclopropanecarboxamide (16).** The compound was synthesized according to procedure **E** using 1-methyl-1*H*-pyrazole-4-boronic acid to give a buff yellow solid: yield 17.3%. The product was purified by CC (DCM/MeOH 100:3 ); mp 254.2-255.3; $^{1}$H NMR (500 MHz, DMSO) δ 10.52 (s, 1H), 8.63 (s, 2H), 8.36 (s, 1H), 8.08 (s, 1H), 7.86 – 7.80 (m, 2H), 7.61 (d, *J* = 1.0 Hz, 1H), 3.86 (s, 3H), 1.87 – 1.74 (m, 1H), 0.92 – 0.78 (m, 4H); $^{13}$C NMR (126 MHz, DMSO) δ172.48, 140.30, 139.77, 139.36, 136.38, 136.14, 134.79, 129.47, 127.91, 123.78, 121.85, 118.52, 117.38, 38.56, 14.54, 7.51; MS (ESI) m/z = 325.10 $(M + H)^+$

**4.1.1.37 *N*-(5-(4-(1-Ethyl-1*H*-pyrazol-4-yl)thiophen-2-yl)pyridine yl)cyclopropanecarboxamide (17).** The compound was synthesized according to procedure **E** using **compound I** to give a light brown solid: yield 17.3%. The product was purified by CC (DCM/MeOH 100:4); mp 240.3-242; $^{1}$H NMR (500 MHz, DMSO) δ 10.55 (s, 1H), 8.64 (s, 2H), 8.37 (s, 1H), 8.15 (s, 1H), 7.89 – 7.81 (m, 2H), 7.61 (d, *J* = 1.0 Hz, 1H), 4.14 (q, *J* = 7.3 Hz, 2H), 1.88 – 1.72 (m, 1H), 1.40 (t, *J* = 7.3 Hz, 3H), 0.93 – 0.82 (m, 4H); $^{13}$C NMR (126 MHz, DMSO)

δ 172.53, 140.31, 139.76, 139.35, 136.25, 134.94, 130.70, 129.54, 126.47, 123.84, 121.83, 118.48, 117.18, 46.31, 15.39, 14.58, 7.56; MS (ESI) m/z = 339.07 $(M + H)^+$

**4.1.1.38 *N*-(5-(4-(1-Propyl-1*H*-pyrazol-4-yl)thiophen-2-yl)pyridin-3-yl)cyclopropanecarboxamide (18).** The compound was synthesized according to procedure **E** using **compound J** to give a white solid: yield 28.9%. The product was purified by CC (DCM/MeOH 100:3); mp 225.5-228.3; $^1$H NMR (500 MHz, DMSO) δ 10.57 (s, 1H), 8.65 (s, 2H), 8.37 (s, 1H), 8.14 (s, 1H), 7.86 (d, *J* = 1.2 Hz, 1H), 7.85 (s, 1H), 7.62 (d, *J* = 1.2 Hz, 1H), 4.07 (t, *J* = 6.9 Hz, 2H), 1.84 – 1.78 (m, 3H), 0.86 (dd, *J* = 5.9, 2.9 Hz, 6H), 0.83 (s, 1H);$^{13}$C NMR (126 MHz, DMSO) δ 172.52, 140.22, 139.74, 139.28, 139.25, 136.31, 134.91, 129.61, 127.13, 123.85, 121.85, 118.48, 117.05, 52.95, 23.14, 14.56, 10.93, 7.55; MS (ESI) m/z = 353.04 $(M + H)^+$

**4.1.1.39 *N*-(5-(4-(1-isopropyl-1*H*-pyrazol-4-yl)thiophen-2-yl)pyridin-3-yl)cyclopropanecarboxamide (19).** The compound was synthesized according to procedure **E** using **compound K** to give a beige solid: yield 24.2%. The product was purified by CC (DCM/MeOH 100:3); mp 198.1-200.6; $^1$H NMR (500 MHz, DMSO) δ 10.57 (s, 1H), 8.66 (s, 2H), 8.38 (s, 1H), 8.20 (s, 1H), 7.86 (d, *J* = 18.6 Hz, 2H), 7.61 (s, 1H), 4.59 – 4.31 (m, 1H), 1.91 – 1.79 (m, 1H), 1.44 (d, *J* = 6.6 Hz, 6H), 0.86 (d, *J* = 4.6 Hz, 4H); $^{13}$C NMR (126 MHz, DMSO) δ 172.49, 140.25, 139.69, 139.30, 136.21, 135.86, 135.04, 129.52, 124.78, 123.85, 121.77, 118.33, 116.89, 53.00, 22.64, 14.54, 7.52; MS (ESI) m/z = 353.26 $(M + H)^+$

### 4.2 Biological Assays.

#### 4.2.1 Protein Kinases and Inhibition Assays.

Human Dyrk1A was expressed and purified as described earlier.[43] Dyrk1B and Clk1 were purchased from Life Technologies (lot no. 877059G, Catalog no. PV4649 and lot no.1095729A, catalog no. PV3315). Woodtide substrate peptide for Dyrk1A and Dyrk1B (KKISGRLSPIMTEQ) and RS repeat substrate peptide for Clk1 (GRSRSRSRSRSRSRSR) were custom synthesized at the Department of Medical Biochemistry and Molecular Biology, Saarland University, Homburg, Germany. Kinase inhibition assays for Dyrk1A, Dyrk1B and Clk1 were performed as described previously, in the presence of 15 μM ATP. [43] The calculated $IC_{50}$ values are representative of at least two independent determinations. The larger panel of kinases shown in Table 3 was screened by the SelectScreen Kinase Profiling Service, Thermo Fisher Scientific, Paisley, U.K.

#### 4.2.2 Cell-Based Assays.

Stock solutions of the inhibitors were prepared in dimethylsulfoxide (DMSO). All effects were compared to vehicle controls which contained DMSO at the respective final concentration in growth medium. Protein kinase activity of endogenous Dyrk1A in HeLa cells was assayed by measuring the phosphorylation of T434 in overexpressed GFP-SF3b1-NT as described previously.[52] Briefly, HeLa cells were transiently transfected in 6-well plates and treated with test compounds for 18 h. Total cellular lysates were subjected to Western blot analysis with the help of a custom-made rabbit antibody for phosphorylated T434 in SF3b1 and a commercial goat antibody for GFP (no. 600-101-215, Rockland Immunochemicals, Gilbertsville, PA, USA). Blots were developed using horseradish peroxidase (HRP)–conjugated secondary antibodies and enhanced chemiluminescent substrates. Signals were quantified using the AIDA Image Analyzer

5.0 program (Raytest, Straubenhardt, Germany). pT434 signals were normalised to total protein levels as determined from GFP immunoreactivity. GraphPad Prism 5.0 (GraphPad Software, La Jolla, CA, USA) was used for non-linear curve fitting (Hill slope -1).

Viability assays were performed using a 96-well pate format (20,000–30,000 cells per well). Cells were cultivated for 3 days before cell viability was assessed with the help of a tetrazolium dye assay (XTT assay, AppliChem GmbH, Darmstadt, Germany).

### 4.3 Physicochemical properties calculation.

Calculation of key physicochemical properties was performed using ACD/Labs software (ACD/ Percepta 2012, Advanced Chemistry Development, Inc) as described previously.[43]

### 4.4 Molecular docking studies.

Molecular docking was performed as previously described using MOE.[53] To model the ATP binding site of Dyrk1B, which has not been crystallized, Met240 in the Dyrk1A crystal structure (PDB entry: 3ANR) was mutated *in silico* to leucine, followed by an energy minimization of the side chain using the rotamer explorer routine embedded in MOE.

### 4.5 Metabolic stability in a cell free assay.

Evaluation of metabolic stability and determination of half-lives were carried out using human S9 fraction as described previously.[44]

**Figures**

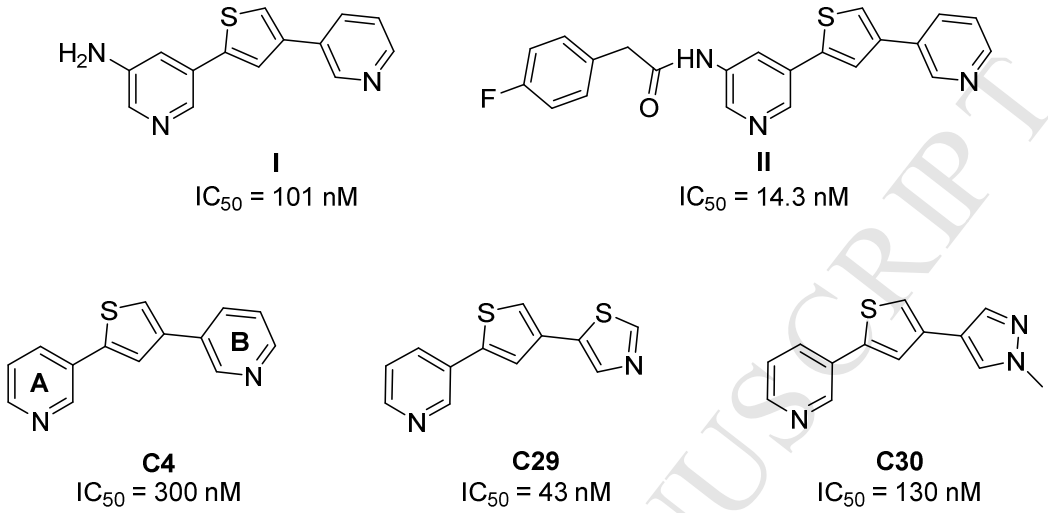


**Fig. 1.** Previously published Dyrk1A inhibitors derived from the basic 2,4-bispyridyl thiophene scaffold C4. The $IC_{50}$ values against Dyrk1A are indicated (determined at 15 µM ATP).

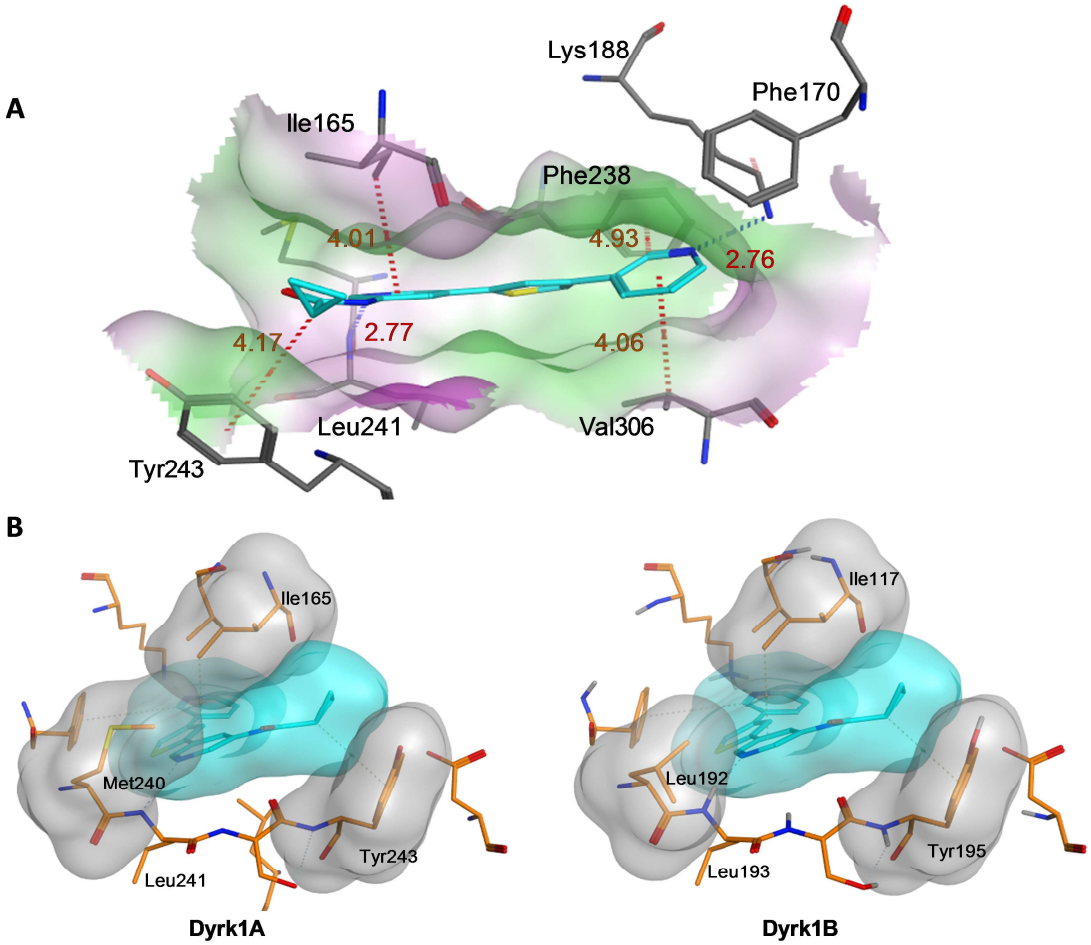


**Fig. 2.** (A) Binding model for the interaction between compound **4b** and the ATP binding pocket of Dyrk1A (PDB code: 3ANR). **4b** (cyan) was docked into the ATP pocket of Dyrk1A using MOE. In the binding model, compound **4b** is anchored between the conserved Lys188 and the hinge region residue Leu241 through two hydrogen bonds with the two pyridine rings. In addition, we found three CH–π interactions involving Lys188, Phe238 and Ile165. The cyclopropyl extension was proven beneficial by performing an extra Van der Waals interaction with the benzene ring of Tyr243. Interactions are indicated by dashed lines (blue; hydrogen bonds, red; CH–π interactions), and distances between the heavy atoms are given in Å. In the color code of the ATP binding pocket surface, green denotes the most lipophilic and magenta the most hydrophilic areas. (B) Met240 in Dyrk1A is expected to perform van der Waals interaction with the pyridine ring that is H-bonded to Leu241 in the Dyrk1A ATP pocket, possibly anchoring the pyridine ring at this position. Interactions with Ile165 additionally stabilize the complex. In contrast, the van der Waals interaction surface to the corresponding Leu192 (right panel, Dyrk1B) is considerably smaller.

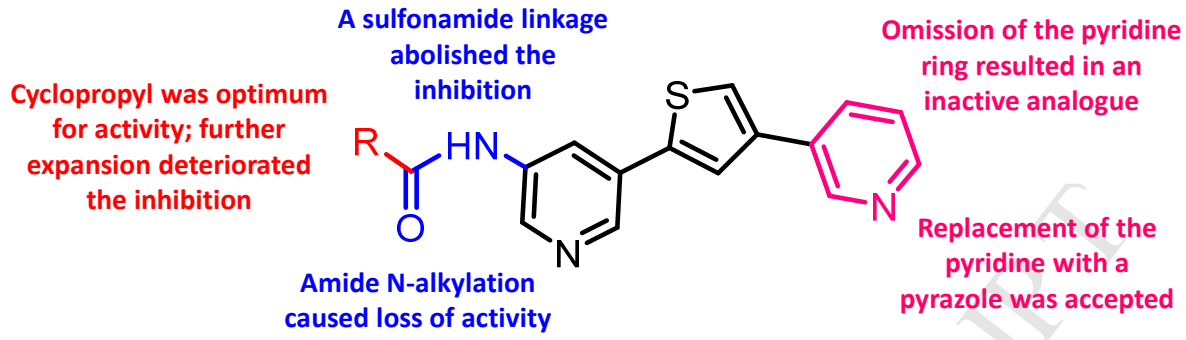


**Fig. 3.** Summary of the structure activity relationship for Dyrk1A inhibition.

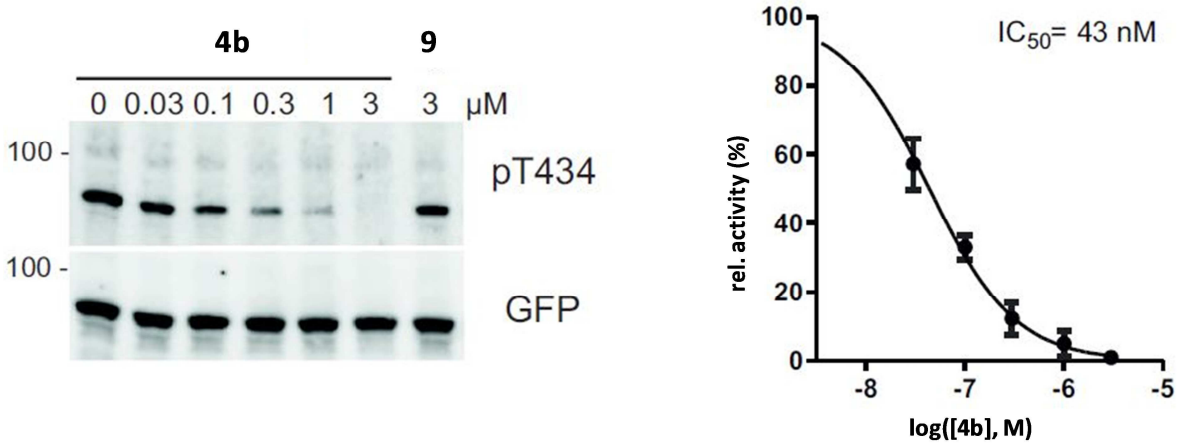


**Fig. 4.** Inhibition of SF3b1 phosphorylation by Dyrk1A inhibition in HeLa cells using **4b**. HeLa cells expressing GFP-SF3b1-NT were treated with the indicated compounds for 18 h at the shown concentrations. Phosphorylation of SF3b1 was quantitated by immunoblotting with pT434 antibody (left panels). Compound **9** from present work was used as a negative control as it did not inhibit Dyrk1A in the primary kinase screening. Quantitative evaluation of the results was performed to calculate the indicated $IC_{50}$ which was deduced from the dose-response curve fitted to the results of three experiments (means ± SEM). All data were standardized to the level of phosphorylation in cells untreated with inhibitors.

## Schemes

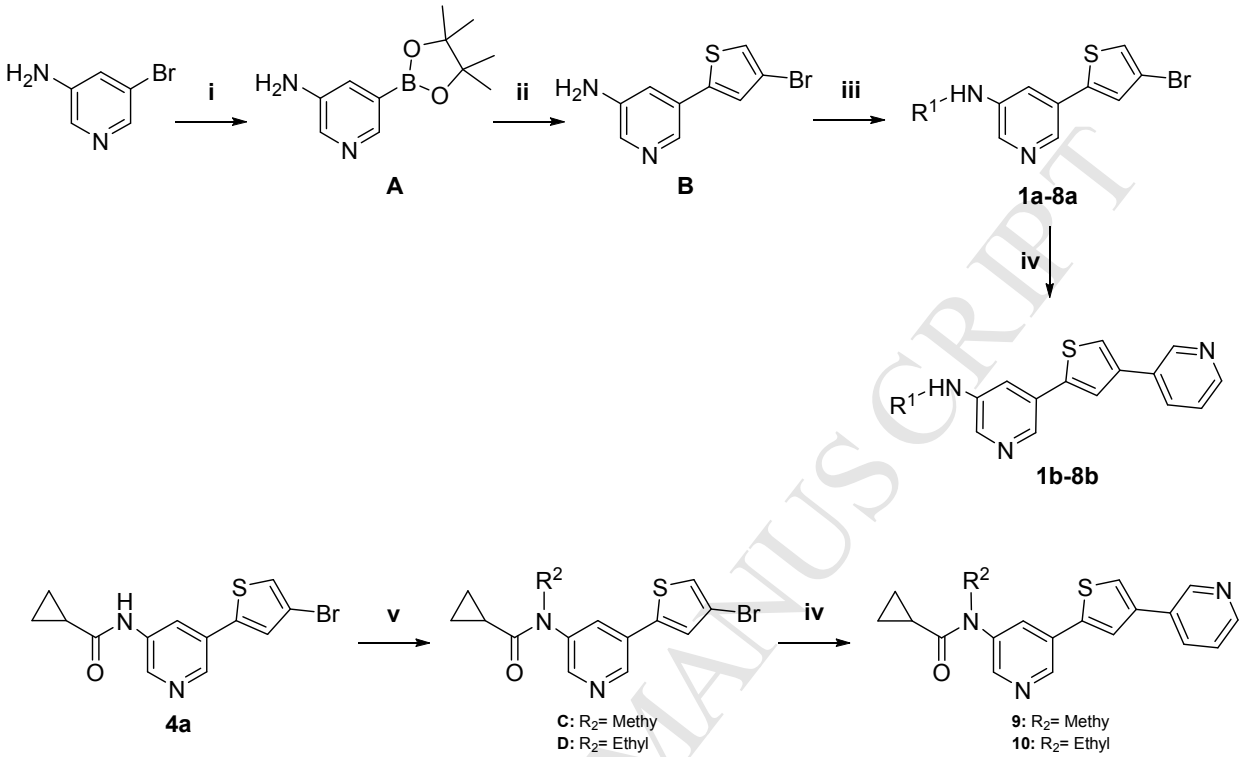


**Scheme 1.** Reagents and conditions: (i) 4 equiv of potassium acetate, 4 equiv bis(pinacolato)diboron, 5 mmol% of Pd(dppf)$Cl_2$ in dioxane, reflux 2 hours; (ii) 4 equiv of $Cs_2CO_3$, 5 mmol% of palladium-tetrakis(triphenylphosphine), 1.2 equiv of 2,4-dibromothiophene in dioxane/water, reflux 3.5 hours; (iii) 1.5 equiv of HBTU (or HATU), 4 equiv of DIPEA, 3 equiv of the appropriate acid in DCM, room temperature, overnight; or 2 equiv of the appropriate sulfonyl chloride in pyridine, 60°C, overnight; (iv) 4 equiv of $Na_2CO_3$, 5 mmol% of Pd(dppf)$Cl_2$, 2 equiv of 3-pyridine boronic acid in dioxane/water, reflux, 2 hours; (v) 10 equiv of KH, 1 equiv of the appropriate alkyl iodide in DMF, room temperature, 2 days.

| No | $R^1$ | No | $R^1$ |
|---|---|---|---|
| **1a** | 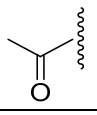 | **5a** | 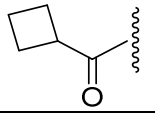 |
| **2a** | 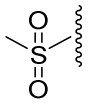 | **6a** | 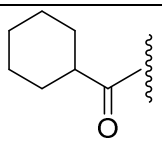 |
| **3a** | 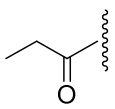 | **7a** | 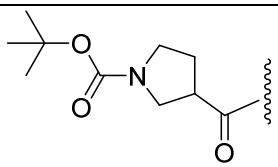 |

| | | | |
|---|---|---|---|
| **4a** | 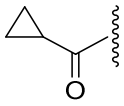 | **8a** | 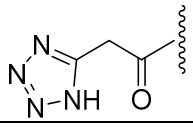 |

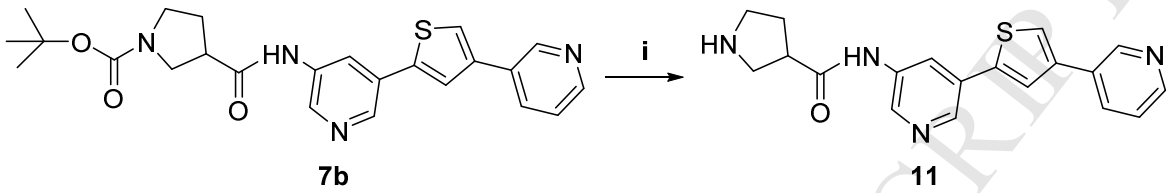


**Scheme 2.** Reagents and conditions: (i) TFA in DCM, room temperature, overnight.

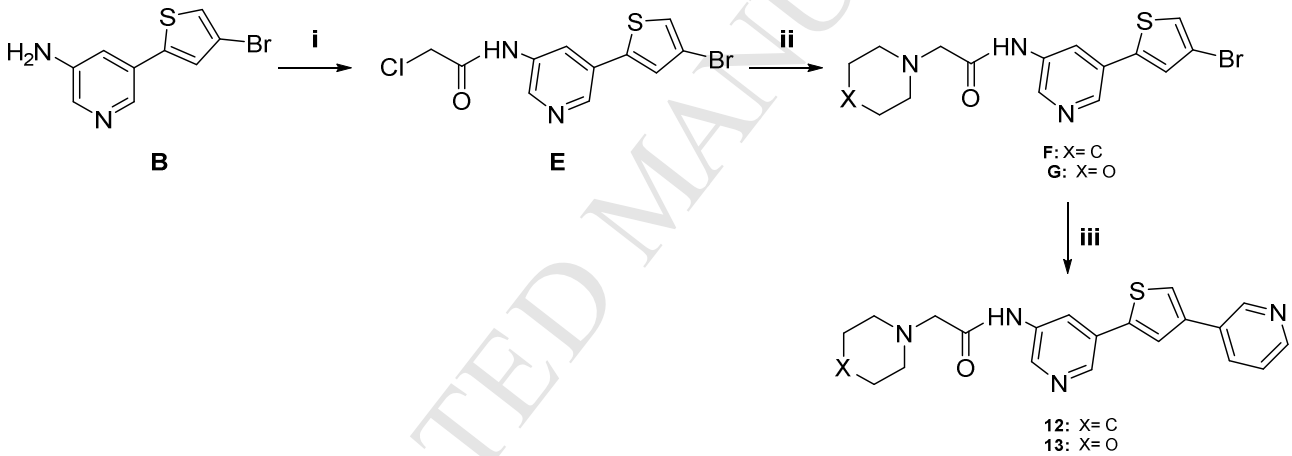


**Scheme 3.** Reagents and conditions: (i) 1.5 equiv of HBTU, 4 equiv of DIPEA, 3 equiv of chloroacetic acid, room temperature, overnight; (ii) 10 equiv of the appropriate alicycle in methanol, reflux, 2 hours; (iii) 4 equiv of $Na_2CO_3$, 5 mmol% of $Pd(dppf)Cl_2$, 2 equiv of 3-pyridine boronic acid in dioxane/water, reflux, 2hours.

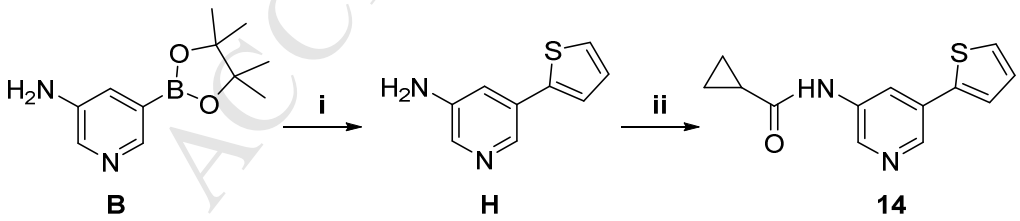


**Scheme 4.** Reagents and conditions: (i) 4 equiv of $Cs_2CO_3$, 5 mmol% of palladium-tetrakis(triphenylphosphine), 1.2 equiv of 2-Bromothiophene in dioxane/water, reflux 3 hours; (ii) 1.5 equiv of HBTU, 4 equiv of DIPEA, 3 equiv cyclopropanecarboxylic acid in DCM, room temperature, overnight.

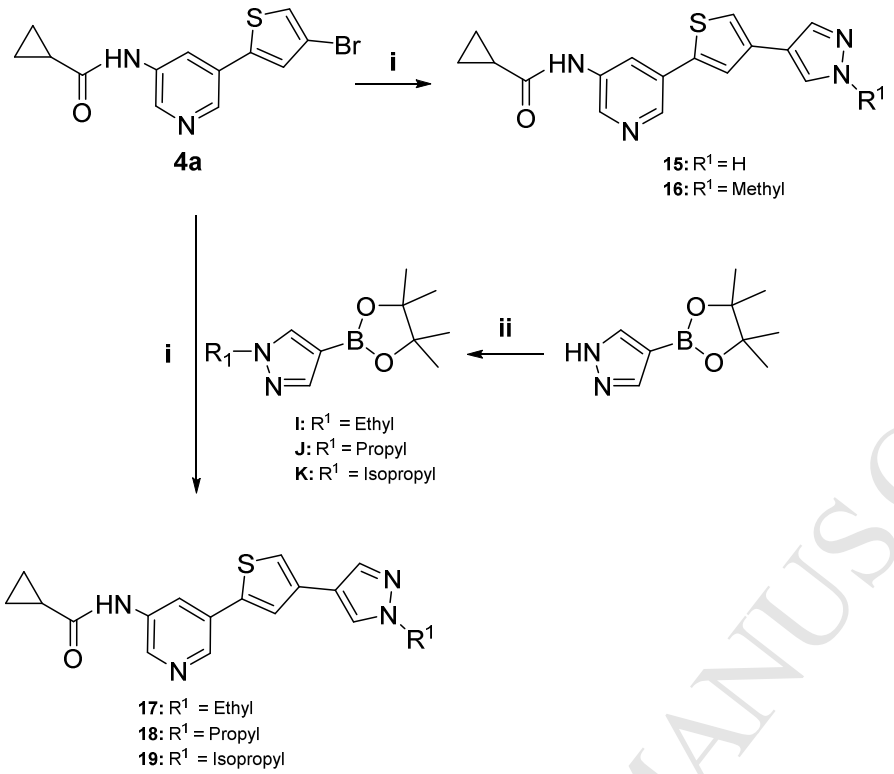


**Scheme 5.** Reagents and conditions: (i) 4 equiv of $Na_2CO_3$, 5 mmol% of $Pd(dppf)Cl_2$, 2 equiv of the appropriate pyrazole boronic acid in dioxane/water, reflux, 2 hours; (ii) 2 equiv of $Cs_2CO_3$, 2 equiv of the appropriate alkyl iodide in acetone, reflux, overnight.

## Tables

**Table 1**

Inhibition of Dyrk1A and Dyrk1B by the (bis)pyridine thiophene derivatives **1b-8b**, **9-14**

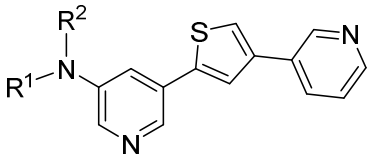

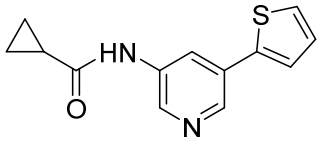

**14**

| Cpd.No. | $R^1$ | $R^2$ | Dyrk1A | | Dyrk1B | |
|---|---|---|---|---|---|---|
| | | | % inhibition at 250 nM[a] | $IC_{50}$ (nM)[a] | % inhibition at 250 nM[a] | $IC_{50}$ (nM)[a] |
| **1b** | 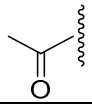 | H | 17.6 | ND | 40.3 | ND |
| **2b** | 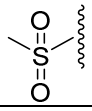 | H | 0 | ND | 23.5 | ND |
| **3b** | 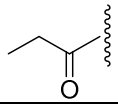 | H | 18.6 | ND | 49.3 | ND |
| **4b** | 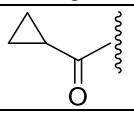 | H | 73.1 | 3.2 | 40 | 72.9 |
| **5b** | 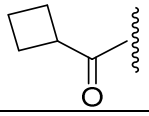 | H | 65.7 | 57.8 | 81 | 218.8 |
| **6b** | 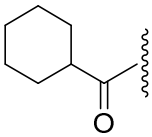 | H | 40.3 | ND | 51 | ND |
| **7b** | 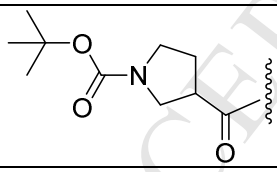 | H | 0 | ND | 34.9 | ND |
| **8b** | 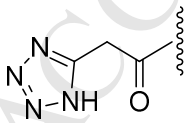 | H | 24.4 | ND | 38.5 | ND |
| **9** | 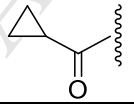 | methyl | 19.4 | ND | 0.9 | ND |
| **10** | 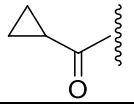 | ethyl | 24.9 | ND | 14.6 | ND |

| | | | | | | |
|---|---|---|---|---|---|---|
| **11** | 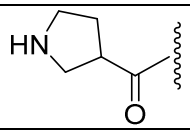 | H | 57.4 | ND | 62.7 | 131.7 |
| **12** | 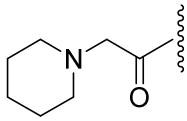 | H | 47.3 | ND | 51.8 | ND |
| **13** | 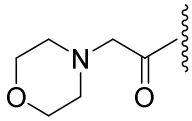 | H | 21.8 | ND | 13.9 | ND |
| **14** | | | 0 | ND | 0 | ND |

[a] Values are mean values of at least two experiments; standard deviation < 9%; the assay was carried out at an ATP conc. of 15 µM; ND: not determined

**Table 2**
Inhibition of Dyrk1A and Dyrk1B by the pyrazol analogues **15-19**

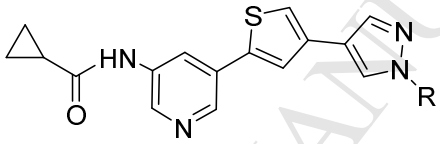

| Cpd.No. | R | Dyrk1A | | Dyrk1B | |
|---|---|---|---|---|---|
| | | % inhibition at 250 nM [a] | $IC_{50}$ (nM) [a] | % inhibition at 250 nM [a] | $IC_{50}$ (nM) [a] |
| **15** | H | 85.7 | 18 | 58.1 | 138 |
| **16** | methyl | 70.4 | 42.6 | 78.6 | 67.1 |
| **17** | ethyl | 78.8 | 29.7 | 57 | ND |
| **18** | propyl | 68 | 76 | 65.7 | 98.8 |
| **19** | isopropyl | 10.1 | ND | 0.7 | ND |

[a] Values are mean values of at least two experiments; standard deviation < 10%; the assay was carried out at an ATP conc. of 15 µM; ND: not determined

**Table 3**
Selectivity profiling of compound **4b**

| kinase | % Inhibition at 1.25 µM[a] ($IC_{50}$)[b] |
|---|---|
| CDK5/p25 | 1 |
| Clk1 | n.d. (270 nM) |
| Clk2 | 21 |
| CK1 delta | 4 |
| Dyrk1A | 89 (3.2 nM) |
| Haspin | 72 (76.3 nM) |
| HIPK1 | 1 |
| MLCK2 | 12.1 |
| TRKB | 8 |
| PIM1 | n.i. |

| | |
|---|---|
| SRPK1 | 2 |
| STK17A | 51.3 |

[a] The screening list was especially composed to include all kinases that were frequently reported as off-targets for diverse chemical classes of Dyrk inhibitors.[30, 43, 54-58] Screenings were performed as a service at Thermo Fisher Scientific at an ATP concentration of 100 µM. n.i., no inhibition. n.d. not determined. Data represent mean values of duplicates that differed by less than 11%. [b] $IC_{50}$ value was determined for inhibition values >60% at an ATP concentration of 15 µM.

**Table 4**

Effect of **1b** and **4b** on HeLa cell growth

| | **1 µM** | **3 µM** | **10 µM** |
|---|---|---|---|
| **4b** | 98±2 | 95±4 | 83±3 |
| **1b** | 99 | 102±3 | 98±3 |
| Staurosporine[a] | 33±4 | | |

Values denote the viability of treated HeLa cells is given in percent relative to control cells treated with vehicle (means of two separate experiments with duplicate measurements ± S.D.). [a] Staurosporine is a known inducer of apoptosis and served as a positive control.

**Table 5**

Calculated physicochemical properties of the most potent compounds **4b** and **15**

| **Cpd.No.** | **MW [gm/mol]** | **logP** | **TPSA [Å$^2$]** | **TPSA [Å$^2$][b]** | **HBD** | **HBA** |
|---|---|---|---|---|---|---|
| **4b** | 321.40 | 2.69 | 83.1 | 54.9 | 1 | 3 |
| **15** | 310.38 | 2.6 | 98.9 | 70.7 | 2 | 3 |
| **C29[a]** | 244.34 | 2.48 | 82.3 | 25.8 | 0 | 2 |

[a] C29 values are shown for comparison (taken from Ref.[43]). [b] Sulphur was not considered for the calculation of TPSA. Ideal ranges for CNS active drugs: MW: 181-427 g/mol, logP 0.4-5.1 (median: 2.8),[45] TPSA < 76 Å$^2$, HBD: 0-1; HBA: 2-3.[48]

**Table 6**

Metabolic stability of **4b** and **15** against human S9 fraction[a]

| **Cpd No.** | **Half-life [min]** |
|---|---|
| **4b** | 144 |
| **15** | 147 |
| **Testosterone[b]** | 8.5 |

[a] 10 mg/ml, $NADP^+$ regenerating system, $MgCl_2$, UDPGA, PAPS, [inhibitor] = 0.3 µM, incubation at 37° C, samples taken at 0, 15, 30, 60, 90 and 120 min, determination of the parent compound by LC-MS/MS. [b] included as a positive control for a rapidly metabolized compound.

**Notes**

The authors declare no competing financial interest.

**Acknowledgements**

The excellent technical assistance by Simone Bamberg-Lember is gratefully acknowledged. The authors would like to thank Prof. Dr. R. W. Hartmann and Prof. Dr. Christian Ducho for generously providing lab facilities to the M.E. group. S.S.D. and M.A.-H. acknowledge The Science & Technology Development Fund in Egypt (STDF) for funding through the GE-SEED, Project 17391. We are also grateful to the DAAD for the travelling support to S.S.D through GradUS Global and GERSS funds. The support by the DAAD in the framework "PPP Ägypten 15" (Project-ID 57190395) to M.E. is highly appreciated. Also, the support by the Deutsche Forschungsgemeinschaft (DFG) (Grant EN381/2-3) to M.E. is greatly acknowledged. We are also thankful for Dr. Mostafa M. Hamed and Mariam G. Tahoun (Helmholtz Institute for Pharmaceutical Research Saarland) for carrying out the metabolic stability studies.

**Abbreviations Used**

AChE, Acetylcholine esterase; AD, Alzheimer's disease; APP, Amyloid precursor protein; ASF, Alternative splicing factor; BBB, Blood brain barier; CC, Column chromatography; CDK, Cyclin dependant kinases; CID, collision induced dissociation; CK, Casein kinase; Clk, cdc like kinae; DS, Down's syndrome; Dyrk, Dual specificity tyrosine regulated kinase; GFP, Green fluorescent protein; HATU, 1-[Bis(dimethylamino)methylene]-1*H*-1,2,3-triazolo[4,5-b]pyridinium 3-oxid hexafluorophosphate; HBA, Hydrogen bond acceptor; HBD, Hydrogen bond donor; HBTU, *N*,*N*,*N*′,*N*′-tetramethyl-*O*-(1*H*-benzotriazol-1-yl)uronium

hexafluorophosphate; HIPK1, Homeodomain-interacting protein kinase 1; $IC_{50}$, Half maximal inhibitory concentration, MLCK2, Myosin light chain kinase 2; NFAT, Nuclear factor of activated T cells; NFT, Neurofibrillary tangles; $Pd(dppf)Cl_2$, [1, 1'-Bis(diphenylphosphino)ferrocene]dichloropalladium(II); PD, Parkinson's disease; PIM1, Proviral integration site for Moloney murine leukemia virus-1; TPSA, Topological polar surface area; TRKB, Tropomyosin receptor kinase B; SF3b1, Splicing factor 3b1; SRPK1, Serine/arginine-rich protein kinase 1; STK17A, Serine/threonine kinase 17A

**References**

[1] B. Smith, F. Medda, V. Gokhale, T. Dunckley, C. Hulme, Recent advances in the design, synthesis, and biological evaluation of selective DYRK1A inhibitors: a new avenue for a disease modifying treatment of Alzheimer's?, ACS Chem Neurosci, 3 (2012) 857-872.

[2] A. Ionescu, F. Dufrasne, M. Gelbcke, I. Jabin, R. Kiss, D. Lamoral-Theys, DYRK1A kinase inhibitors with emphasis on cancer, Mini Rev Med Chem, 12 (2012) 1315-1329.

[3] W. Becker, Y. Weber, K. Wetzel, K. Eirmbter, F.J. Tejedor, H.G. Joost, Sequence characteristics, subcellular localization, and substrate specificity of DYRK-related kinases, a novel family of dual specificity protein kinases, J Biol Chem, 273 (1998) 25893-25902.

[4] H. Kentrup, W. Becker, J. Heukelbach, A. Wilmes, A. Schurmann, C. Huppertz, H. Kainulainen, H.G. Joost, Dyrk, a dual specificity protein kinase with unique structural features whose activity is dependent on tyrosine residues between subdomains VII and VIII, J Biol Chem, 271 (1996) 3488-3495.

[5] S. Himpel, P. Panzer, K. Eirmbter, H. Czajkowska, M. Sayed, L.C. Packman, T. Blundell, H. Kentrup, J. Grotzinger, H.G. Joost, W. Becker, Identification of the autophosphorylation sites and characterization of their effects in the protein kinase DYRK1A, Biochem J, 359 (2001) 497-505.

[6] J. Guimera, C. Casas, C. Pucharcos, A. Solans, A. Domenech, A.M. Planas, J. Ashley, M. Lovett, X. Estivill, M.A. Pritchard, A human homologue of Drosophila minibrain (MNB) is expressed in the neuronal regions affected in Down syndrome and maps to the critical region, Hum Mol Genet, 5 (1996) 1305-1310.

[7] F.J. Tejedor, B. Hammerle, MNB/DYRK1A as a multiple regulator of neuronal development, FEBS J, 278 (2011) 223-235.

[8] J. Wegiel, W. Kaczmarski, M. Barua, I. Kuchna, K. Nowicki, K.C. Wang, S.M. Yang, J. Frackowiak, B. Mazur-Kolecka, W.P. Silverman, B. Reisberg, I. Monteiro, M. de Leon, T. Wisniewski, A. Dalton, F. Lai, Y.W. Hwang, T. Adayev, F. Liu, K. Iqbal, I.G. Iqbal, C.X. Gong, Link between DYRK1A overexpression and several-fold enhancement of neurofibrillary degeneration with 3-repeat tau protein in Down syndrome, J Neuropathol Exp Neurol, 70 (2011) 36-50.

[9] W. Becker, U. Soppa, F.J. Tejedor, DYRK1A: a potential drug target for multiple Down syndrome neuropathologies, CNS Neurol Disord Drug Targets, 13 (2014) 26-33.

[10] F. Liu, B. Li, E.J. Tung, I. Grundke-Iqbal, K. Iqbal, C.X. Gong, Site-specific effects of tau phosphorylation on its microtubule assembly activity and self-aggregation, Eur J Neurosci, 26 (2007) 3429-3436.

[11] F. Liu, Z. Liang, J. Wegiel, Y.W. Hwang, K. Iqbal, I. Grundke-Iqbal, N. Ramakrishna, C.X. Gong, Overexpression of Dyrk1A contributes to neurofibrillary degeneration in Down syndrome, FASEB J, 22 (2008) 3224-3233.

[12] Y.L. Woods, P. Cohen, W. Becker, R. Jakes, M. Goedert, X. Wang, C.G. Proud, The kinase DYRK phosphorylates protein-synthesis initiation factor eIF2Bepsilon at Ser539 and the microtubule-associated protein tau at Thr212: potential role for DYRK as a glycogen synthase kinase 3-priming kinase, Biochem J, 355 (2001) 609-615.

[13] J. Wegiel, C.X. Gong, Y.W. Hwang, The role of DYRK1A in neurodegenerative diseases, FEBS J, 278 (2011) 236-245.

[14] S.R. Ryoo, H.J. Cho, H.W. Lee, H.K. Jeong, C. Radnaabazar, Y.S. Kim, M.J. Kim, M.Y. Son, H. Seo, S.H. Chung, W.J. Song, Dual-specificity tyrosine(Y)-phosphorylation regulated

kinase 1A-mediated phosphorylation of amyloid precursor protein: evidence for a functional link between Down syndrome and Alzheimer's disease, J Neurochem, 104 (2008) 1333-1344.

[15] E.J. Kim, J.Y. Sung, H.J. Lee, H. Rhim, M. Hasegawa, T. Iwatsubo, S. Min do, J. Kim, S.R. Paik, K.C. Chung, Dyrk1A phosphorylates alpha-synuclein and enhances intracellular inclusion formation, J Biol Chem, 281 (2006) 33250-33257.

[16] J.H. Sitz, K. Baumgartel, B. Hammerle, C. Papadopoulos, P. Hekerman, F.J. Tejedor, W. Becker, B. Lutz, The Down syndrome candidate dual-specificity tyrosine phosphorylation-regulated kinase 1A phosphorylates the neurodegeneration-related septin 4, Neuroscience, 157 (2008) 596-605.

[17] M. Ihara, H. Tomimoto, H. Kitayama, Y. Morioka, I. Akiguchi, H. Shibasaki, M. Noda, M. Kinoshita, Association of the cytoskeletal GTP-binding protein Sept4/H5 with cytoplasmic inclusions found in Parkinson's disease and other synucleinopathies, J Biol Chem, 278 (2003) 24095-24102.

[18] M. Ihara, N. Yamasaki, A. Hagiwara, A. Tanigaki, A. Kitano, R. Hikawa, H. Tomimoto, M. Noda, M. Takanashi, H. Mori, N. Hattori, T. Miyakawa, M. Kinoshita, Sept4, a component of presynaptic scaffold and Lewy bodies, is required for the suppression of alpha-synuclein neurotoxicity, Neuron, 53 (2007) 519-533.

[19] E. Im, K.C. Chung, Dyrk1A phosphorylates parkin at Ser-131 and negatively regulates its ubiquitin E3 ligase activity, J Neurochem, 134 (2015) 756-768.

[20] J. Shi, T. Zhang, C. Zhou, M.O. Chohan, X. Gu, J. Wegiel, J. Zhou, Y.W. Hwang, K. Iqbal, I. Grundke-Iqbal, C.X. Gong, F. Liu, Increased dosage of Dyrk1A alters alternative splicing factor (ASF)-regulated alternative splicing of tau in Down syndrome, J Biol Chem, 283 (2008) 28660-28669.

[21] X. Yin, N. Jin, J. Gu, J. Shi, J. Zhou, C.X. Gong, K. Iqbal, I. Grundke-Iqbal, F. Liu, Dual-specificity tyrosine phosphorylation-regulated kinase 1A (Dyrk1A) modulates serine/arginine-rich protein 55 (SRp55)-promoted Tau exon 10 inclusion, J Biol Chem, 287 (2012) 30497-30506.

[22] W. Qian, H. Liang, J. Shi, N. Jin, I. Grundke-Iqbal, K. Iqbal, C.X. Gong, F. Liu, Regulation of the alternative splicing of tau exon 10 by SC35 and Dyrk1A, Nucleic Acids Res, 39 (2011) 6161-6171.

[23] V. La Cognata, V. D'Agata, F. Cavalcanti, S. Cavallaro, Splicing: is there an alternative contribution to Parkinson's disease?, Neurogenetics, 16 245-263.

[24] Z. Zhou, X.D. Fu, Regulation of splicing by SR proteins and SR protein-specific kinases, Chromosoma, 122 (2013) 191-207.

[25] K. de Graaf, H. Czajkowska, S. Rottmann, L.C. Packman, R. Lilischkis, B. Luscher, W. Becker, The protein kinase DYRK1A phosphorylates the splicing factor SF3b1/SAP155 at Thr434, a novel in vivo phosphorylation site, BMC Biochem, 7 (2006) 7.

[26] X. Yin, N. Jin, J. Shi, Y. Zhang, Y. Wu, C.X. Gong, K. Iqbal, F. Liu, Dyrk1A overexpression leads to increase of 3R-tau expression and cognitive deficits in Ts65Dn Down syndrome mice, Sci Rep, 7 (2017) 12.

[27] D. Toiber, G. Azkona, S. Ben-Ari, N. Toran, H. Soreq, M. Dierssen, Engineering DYRK1A overdosage yields Down syndrome-characteristic cortical splicing aberrations, Neurobiol Dis, 40 (2010) 348-359.

[28] J. Bain, L. Plater, M. Elliott, N. Shpiro, C.J. Hastie, H. McLauchlan, I. Klevernic, J.S. Arthur, D.R. Alessi, P. Cohen, The selectivity of protein kinase inhibitors: a further update, Biochem J, 408 (2007) 297-315.

[29] Y. Ogawa, Y. Nonaka, T. Goto, E. Ohnishi, T. Hiramatsu, I. Kii, M. Yoshida, T. Ikura, H. Onogi, H. Shibuya, T. Hosoya, N. Ito, M. Hagiwara, Development of a novel selective inhibitor of the Down syndrome-related kinase Dyrk1A, Nat Commun, 1 (2010) 86.

[30] T. Tahtouh, J.M. Elkins, P. Filippakopoulos, M. Soundararajan, G. Burgy, E. Durieu, C. Cochet, R.S. Schmid, D.C. Lo, F. Delhommel, A.E. Oberholzer, L.H. Pearl, F. Carreaux, J.P. Bazureau, S. Knapp, L. Meijer, Selectivity, cocrystal structures, and neuroprotective properties of leucettines, a family of protein kinase inhibitors derived from the marine sponge alkaloid leucettamine B, J Med Chem, 55 (2012) 9312-9330.

[31] S. Coutadeur, H. Benyamine, L. Delalonde, C. de Oliveira, B. Leblond, A. Foucourt, T. Besson, A.S. Casagrande, T. Taverne, A. Girard, M.P. Pando, L. Desire, A novel DYRK1A (dual specificity tyrosine phosphorylation-regulated kinase 1A) inhibitor for the treatment of Alzheimer's disease: effect on Tau and amyloid pathologies in vitro, J Neurochem, 133 (2015) 440-451.

[32] R. Meine, W. Becker, H. Falke, L. Preu, N. Loaec, L. Meijer, C. Kunick, Indole-3-Carbonitriles as DYRK1A Inhibitors by Fragment-Based Drug Design, Molecules, 23 (2018).

[33] E. Friedman, Mirk/Dyrk1B in cancer, J Cell Biochem, 102 (2007) 274-279.

[34] K. Jin, S. Park, D.Z. Ewton, E. Friedman, The survival kinase Mirk/Dyrk1B is a downstream effector of oncogenic K-ras in pancreatic cancer, Cancer Res, 67 (2007) 7247-7255.

[35] E. Friedman, The Kinase Mirk/dyrk1B: A Possible Therapeutic Target in Pancreatic Cancer, Cancers (Basel), 2 (2010) 1492-1512.

[36] M. He, J. Gu, J. Zhu, X. Wang, C. Wang, C. Duan, Y. Ni, X. Lu, J. Li, Up-regulation of Dyrk1b promote astrocyte activation following lipopolysaccharide-induced neuroinflammation, Neuropeptides, 69 (2018) 7.

[37] R. Medeiros, F.M. LaFerla, Astrocytes: conductors of the Alzheimer disease neuroinflammatory symphony, Exp Neurol, 239 (2013) 133-138.

[38] M. Belanger, P.J. Magistretti, The role of astroglia in neuroprotection, Dialogues Clin Neurosci, 11 (2009) 281-295.

[39] R. Mathur, P.G. Ince, T. Minett, C.J. Garwood, P.J. Shaw, F.E. Matthews, C. Brayne, J.E. Simpson, S.B. Wharton, A reduced astrocyte response to beta-amyloid plaques in the ageing brain associates with cognitive impairment, PLoS One, 10 (2015) e0118463.

[40] S. Abu Jhaisha, E.W. Widowati, I. Kii, R. Sonamoto, S. Knapp, C. Papadopoulos, W. Becker, DYRK1B mutations associated with metabolic syndrome impair the chaperone-dependent maturation of the kinase domain, Sci Rep, 7 (2017) 6432.

[41] P.I. Duncan, D.F. Stojdl, R.M. Marius, K.H. Scheit, J.C. Bell, The Clk2 and Clk3 dual-specificity protein kinases regulate the intranuclear distribution of SR proteins and influence pre-mRNA splicing, Exp Cell Res, 241 (1998) 300-308.

[42] J.M. Higgins, Haspin: a newly discovered regulator of mitotic chromosome behavior, Chromosoma, 119 (2010) 137-147.

[43] C. Schmitt, D. Kail, M. Mariano, M. Empting, N. Weber, T. Paul, R.W. Hartmann, M. Engel, Design and synthesis of a library of lead-like 2,4-bisheterocyclic substituted thiophenes as selective Dyrk/Clk inhibitors, PLoS One, 9 (2014) e87851.

[44] S.S. Darwish, M. Abdel-Halim, M. Salah, A.H. Abadi, W. Becker, M. Engel, Development of Novel 2,4-Bispyridyl Thiophenes as Highly Potent and Selective Dyrk1A Inhibitors. Part I: Benzamide and Benzylamide Derivatives, Eur J Med Chem, (2018).

[45] T.T. Wager, R.Y. Chandrasekaran, X. Hou, M.D. Troutman, P.R. Verhoest, A. Villalobos, Y. Will, Defining desirable central nervous system drug space through the alignment of

molecular properties, in vitro ADME, and safety attributes, ACS Chem Neurosci, 1 (2010) 420-434.

[46] B. Baum, L. Muley, M. Smolinski, A. Heine, D. Hangauer, G. Klebe, Non-additivity of functional group contributions in protein-ligand binding: a comprehensive study by crystallography and isothermal titration calorimetry, J Mol Biol, 397 (2010) 1042-1054.

[47] B.R. Beno, K.S. Yeung, M.D. Bartberger, L.D. Pennington, N.A. Meanwell, A Survey of the Role of Noncovalent Sulfur Interactions in Drug Design, J Med Chem, 58 (2015) 4383-4438.

[48] A.K. Ghose, T. Herbertz, R.L. Hudkins, B.D. Dorsey, J.P. Mallamo, Knowledge-Based, Central Nervous System (CNS) Lead Selection and Lead Optimization for CNS Drug Discovery, ACS Chem Neurosci, 3 (2012) 50-68.

[49] D. Huang, S.F. Poon, D.F. Chapman, J. Chung, M. Cramer, T.S. Reger, J.R. Roppe, L. Tehrani, N.D. Cosford, N.D. Smith, 2-(2-[3-(pyridin-3-yloxy)phenyl]-2H-tetrazol-5-yl) pyridine: a highly potent, orally active, metabotropic glutamate subtype 5 (mGlu5) receptor antagonist, Bioorg Med Chem Lett, 14 (2004) 5473-5476.

[50] O. Fedorov, K. Huber, A. Eisenreich, P. Filippakopoulos, O. King, A.N. Bullock, D. Szklarczyk, L.J. Jensen, D. Fabbro, J. Trappe, U. Rauch, F. Bracher, S. Knapp, Specific CLK inhibitors from a novel chemotype for regulation of alternative splicing, Chem Biol, 18 (2011) 67-76.

[51] G.D. Cuny, N.P. Ulyanova, D. Patnaik, J.F. Liu, X. Lin, K. Auerbach, S.S. Ray, J. Xian, M.A. Glicksman, R.L. Stein, J.M. Higgins, Structure-activity relationship study of beta-carboline derivatives as haspin kinase inhibitors, Bioorg Med Chem Lett, 22 (2012) 2015-2019.

[52] N. Gockler, G. Jofre, C. Papadopoulos, U. Soppa, F.J. Tejedor, W. Becker, Harmine specifically inhibits protein kinase DYRK1A and interferes with neurite formation, FEBS J, 276 (2009) 6324-6337.

[53] A.K. ElHady, M. Abdel-Halim, A.H. Abadi, M. Engel, Development of Selective Clk1 and -4 Inhibitors for Cellular Depletion of Cancer-Relevant Proteins, J Med Chem, 60 (2017) 5377-5391.

[54] J. Bain, H. McLauchlan, M. Elliott, P. Cohen, The specificities of protein kinase inhibitors: an update, Biochem J, 371 (2003) 199-204.

[55] T. Anastassiadis, S.W. Deacon, K. Devarajan, H. Ma, J.R. Peterson, Comprehensive assay of kinase catalytic activity reveals features of kinase inhibitor selectivity, Nat Biotechnol, 29 (2011) 1039-1045.

[56] M.A. Pagano, J. Bain, Z. Kazimierczuk, S. Sarno, M. Ruzzene, G. Di Maira, M. Elliott, A. Orzeszko, G. Cozza, F. Meggio, L.A. Pinna, The selectivity of inhibitors of protein kinase CK2: an update, Biochem J, 415 (2008) 353-365.

[57] C. Schmitt, P. Miralinaghi, M. Mariano, R.W. Hartmann, M. Engel, Hydroxybenzothiophene Ketones Are Efficient Pre-mRNA Splicing Modulators Due to Dual Inhibition of Dyrk1A and Clk1/4, ACS Med Chem Lett, 5 (2014) 963-967.

[58] G.D. Cuny, M. Robin, N.P. Ulyanova, D. Patnaik, V. Pique, G. Casano, J.F. Liu, X. Lin, J. Xian, M.A. Glicksman, R.L. Stein, J.M. Higgins, Structure-activity relationship study of acridine analogs as haspin and DYRK2 kinase inhibitors, Bioorg Med Chem Lett, 20 (2010) 3491-3494.

Highlights

- A series of 2,4-bispyridinyl thiophenes alkyl amide derivatives were synthesized
- Cyclopropyl amide extension (4b) was discovered as a key modification showing excellent Dyrk1A inhibition ($IC_{50}$ = 3.2 nM)
- 4b exhibited a remarkable cellular potency with an $IC_{50}$ of 43 nM
- Potent compounds exhibited enhancement in metabolic stability as well as high probability of CNS penetration